INSTITUTO SUPERIOR TÉCNICO

FACULDADE DE MEDICINA DE LISBOA

Ionic Atrial Remodelling in Atrial Fibrillation and its Effect in the Cardiac Action Potential

Luís Filipe Gameiro Matos

Master Thesis in

Biomedical Engineering

Advisors:

Raúl Carneiro Martins

Luís Silva Carvalho

Jury:

Fernando Lopes da Silva

Raúl Carneiro Martins

Maria Isabel Rocha

Fernando Tim-Tim Janeiro

Lisboa, May 2009

Dedicated to the memory of

Professor Luís Silva Carvalho

Acknowledgments

First of all I would like to thank my thesis advisor and mentor in this project, Professor Luís Silva Carvalho. He was the first to motivate me for this project, and a source of valuable insight and discussion. Most of all I thank my fellow working colleagues from the Physiology Department. Without their help, intellectual stimulation and overall dedication this endeavor would not have been possible. I would like to thank my advisor Raúl Martins for the constant availability for debate and clarification, for the useful information and insight provided during the entire project. I cheerfully thank my family for offering me the opportunity to study and for all their support and encouragement.

I'm thankful to Marta Dias for her help, support and affection, and also to my colleagues of the late working hours for their intellectual stimuli and friendship.

I would like to acknowledge the role of the two institutions that played a major role in my superior education, the Instituto Superior Técnico and the Faculdade de Medicina de Lisboa, where I completed my studies and gathered the knowledge in the most diverse fields of engineering and medical sciences, which was essential in the completion of this study. I also would like to thank Dr. João Paulo Gomes and his team from the National Institute of Health Ricardo Jorge, for their contribution on the gene expression analysis and all the valuable information on the subject. In addition I would like to remark that the genetic expression analysis and results are part of a broader study on atrial fibrillation conducted by Dr. Mário Oliveira and integrated in his doctoral thesis. Such data were used in this thesis for comparison with the signal analysis results. And finally I would like to acknowledge the support of St. Jude Medical foundation in funding my participation in this project.

Resumo

A fibrilhação auricular (AF) é uma arritmia muito comum, especialmente entre os idosos, que consiste na activação caótica e ineficiente das aurículas, originando assim, um ritmo ventricular irregular. O progressivo envelhecimento da população justifica uma crescente preocupação e consequente interesse no estudo dos mecanismos fisiológicos que estão na origem desta doença, de forma a desenvolver tratamentos mais eficazes ou mesmo terapias de prevenção. Este trabalho pretende caracterizar os indícios iniciais da remodelagem auricular associada à AF, os seus efeitos nas propriedades genéticas e electrofisiológicas do coração de forma a compreender melhor a patofisiologia desta doença. Para tal apresenta-se uma nova abordagem à análise dos sinais eléctricos cardíacos recorrendo a um algoritmo iterativo de interpolação, baseado no compromisso de Levenberg-Marquardt, que modela o sinal auricular usando um conjunto de funções gaussianas generalizadas. Estes sinais foram registados durante experiências em modelos animais, em que se estimula a aurícula direita de forma a simular o padrão caótico de activação auricular que ocorre durante a AF. No final foram recolhidas amostras de tecido cardíaco para análise dos níveis de expressão de genes que codificam vários canais iónicos cardíacos. Os resultados da análise de sinal foram relacionados com as alterações de expressão genética de forma a identificar uma relação causal entre elas.

Palavras Chave: Fibrilhação auricular, Remodelagem auricular, Canais iónicos, Expressão genética, Levenberg-Marquardt, Gaussianas generalizadas.

Abstract

Atrial fibrillation (AF) is the most common sustained arrhythmia in humans, especially in the elderly; it is characterized by rapid ineffective atrial activity with irregular ventricular contractions. The increasing elderly population justifies the growing interest in the underlying mechanisms and the investigation of prophylactic treatment of this disease. This project aims to characterize the early stages of atrial remodelling and its effects on the properties of the heart, at the genetic and electrophysiological levels, in order to clarify some of the pathophysiological effects of AF. A novel approach was used to analyse the atrial electrical signals, by means of an iterative fitting algorithm based on the Levenberg-Marquardt compromise that models the signal using a set of generalized Gauss functions.

An extensive experimental approach was devised, using rapid atrial electrical stimulation in laboratory animals to simulate the chaotic activation pattern of AF. During these experiments the electrical activity of the heart was monitored and samples of atrial tissue were collected. These samples were processed for RNA quantification of specific genes encoding cardiac ion channels. The atrial recordings were correlated with the changes in expression of ion channels in the atrial tissue, to identify causality between them.

Keywords: Atria fibrillation, remodelling, Ion channles, Gene expression, Levenberg-Marquardt, Generalized Gauss functions.

Contents

Acknowledgments **iii**

Resumo **v**

Abstract **vii**

Introduction **1**

1 Atrial Fibrillation **5**

1.1 Normal cardiac activation 6

1.2 Pathophysiology of AF 9

1.3 Atrial Fibrillation and Autonomic Nervous System 11

1.3.1 Autonomic cardiovascular control 12

1.4 Ionic remodelling in Atrial Fibrillation 13

2 Electrocardiogram and Cardiac Potentials **19**

3 Materials and Methods **27**

3.1 Animal Experimental Model 27

3.2 Gene Expression Analysis 28

3.2.1 Sample Preparation 30

3.2.2 RNA Extraction 30

3.2.3 Reverse transcription reaction (RT) 30

3.2.4 Real-time Quantitation Assays for Gene Expression 31

3.3 Data Analysis 32
3.3.1 Gradient Method 35
3.3.2 Gauss-Newton Method 36
3.3.3 Levenberg-Marquardt Compromise 38
3.3.4 Computational Algorithm 40

4 Results **43**
4.1 Gene Expression Analysis 43
4.2 Signal Measurements 48
4.3 Data Analysis 49

5 Discussion **53**
5.1 Gene Expression Analysis 53
5.2 Signal Measurements 58
5.3 Signal Analysis 59

A Bioelectricity **71**
A.1 Cellular Electrophysiology 71
A.1.1 Ionic Equilibrium and Resting Membrane Potential 72
A.1.2 Generation and Conduction of Action Potentials 74

B Autonomic Nervous System **77**
B.1 Sympathetic nervous system 80
B.2 Parasympathetic nervous system 81
B.3 Autonomic Cardiovascular Control 82

List of Figures

1.1 Cardiac Action Potential. [3] 7

1.2 Cardiac Action Potential Currents. [3] 8

2.1 A) Sketch of the injury potential; B) Sketch of the action potential obtained through the injury technique. [28] 20

2.2 Electrocardiogram, Electrogram and MAP. [28] 21

2.3 Intracellular action potential and Monophasic action potential. [30] 22

2.4 Origin of the MAP. [37] 23

2.5 Unipolar MAP. [37] 25

3.1 Computational algorithm scheme 41

4.1 Right Atria Gene Expression Results 44

4.2 Left Atria Gene Expression Results 44

4.3 Right Atria Gene Expression Results 45

4.4 Left Atria Gene Expression Results 46

4.5 Examples of measured MAP signals 48

4.6 Examples of measured MAP signals 49

4.7 Templates 49

4.8 Fitted Model 50

4.9 Right Atria Parameter Changes 51

4.10 Right Atria Parameter Changes in log scale 51

4.11 Right Atrium signal and fit model before and after 4 hours of pacing . . . 51

A.1 Ion transporters [48]. 72

A.2 Action Potential Generation [49]. 75

A.3 Action Potential Propagation [50]. 76

B.1 Autonomic Nervous System [50]. 78

Introduction

Atrial fibrillation induces a series of biochemical and electrophysiological changes within the atrial tissue in a process known as atrial remodelling, which is the central subject in this study. These changes are a consequence of AF and may initially be a compensatory mechanism to the increased rhythm of AF but soon become a contributing factor to the recurrence of the disease. AF is a complex condition that does not derive from a steady abnormality, but instead from a pathological interplay of several dynamic systems. In that sense, this study adopts a multiscale approach, were several factors ranging from genes expression, passing through cell electrical activity, organ and respective control system were investigated and integrated in a model for the disease. Knowledge attained in this study about the physiological system involved in the genesis and progression of AF can contribute to a better understanding of the disease, and to the development of new preventive and treatment strategies. The pathophysiology of AF is currently a very wide field of study where several hypotheses are being considered and a significant number of contributing factors have already been identified. The objective of this study is to correlate and clarify the electrophysiological and biochemical mechanisms underlying the phenomena of atrial remodelling during AF. To pursue this goal, a novel signal analysis approach was implemented to model and extract the subtle changes induced in the atrial electrical signal by rapid atrial stimulation. This approach uses the Levenberg-Marquardt compromise to iteratively fit a parametric model to the measured data. The model used is based on a set of generalized Gauss functions, each defined by five parameters. The hypotheses is that this signal analysis method can be used as a tool to evaluate underlying molecular mechanisms regarding the changes in expression levels of membrane ion channels. If confirmed, the method can be used in the clinical environment as a practical and affordable tool to evaluate the extent of atrial remodelling in AF patients.

This project, as a Biomedical engineering project combines a multitude of engineering and medical research specialties as tools to investigate an idea. As far apart as they may seem, gene expression analysis, electrophysiology or non-linear fit algorithms, they all

will be used in this study, combined as tools to investigate the mechanisms of atrial fibrillation. The multidisciplinary dimension of this project enabled the collaboration of several research institutes, namely the Physiology Institute of the Medical Faculty of Lisbon, coordinator of the project and where the animal experiments were conducted, the Telecommunications Institute of the Instituto Superior Técnico, that contributed with the signal analysis algorithms and the National Health Institute Dr. Ricardo Jorge, responsible for the gene expression analysis.

Chapter 1

Atrial Fibrillation
From Genetics to Signals

Atrial fibrillation (AF) is the most common sustained arrhythmia in humans; it is characterized by rapid ineffective atrial activity with irregular ventricular contractions.
AF occurs in approximately 0.4% to 1.0% of the general population, and it affects more than 2 million people in the United States annually. Its prevalence increases with age, and up to 10% of the population older than 80 years has been diagnosed with AF at some point [1].
Potential complications include stroke, congestive heart failure, tachycardia-induced cardiomyopathy, systemic thromboembolic complications, decreased exercise capacity and impaired ventricular function, which are associated with reduced quality of life and significant health care costs. After adjusting for underlying cardiac conditions, AF is associated with a 1.5-fold to 1.9-fold increase in risk of mortality in both men and women across a wide spectrum of ages.

Patients suffering from cardiac arrhythmias consume a significant proportion of medical resources. Of all the supraventricular tachyarrhythmias, AF is by far the most common and the most important. Rhythm disturbances, mainly AF and flutter, also represent the major cause of patient morbidity and hospital costs following routine cardiac operations. The incidence is about 30% after coronary bypass surgery and up to 48% after aortic valve replacements. The ever growing numbers justify the importance of AF and the growing interest in the underlying mechanisms and the investigation of prophylactic treatment of AF, especially with the projected growth of the elderly population.
Atrial fibrillation occurs when the electrical impulses in the atria degenerate from their

usual organized pattern into a rapid chaotic pattern. This disruption results in an irregular and often rapid heartbeat that is classically described as “irregularly irregular” and is due to the unpredictable conduction of these disordered impulses across the atrioventricular node and to the ventricles.
Atrial fibrillation usually develops because of another disease state, often accompanying left atrial enlargement and mitral valve calcification in patients over 60 years of age and commonly complicating cardiac surgery and acute myocardial infarction. Increasing age, heart failure, smoking, diabetes, hypertension, male gender, left ventricular hypertrophy, myocardial infarction and valvular heart disease are risk factors for the development of AF [2].

1.1 Normal cardiac activation

AF occurs when the orderly succession of atrial electrical activation, conduction and contraction is disrupted either by factors intrinsic to the heart or by external stimuli.
The normal mechanical functioning of the mammalian heart depends on proper electrical organization, reflected in the sequential activation of the specialized pacemaker regions of the heart and in the propagation of activity through the atria and ventricles. Myocardial electrical activity is attributed to the synchronous generation of action potentials in individual cardiac cells, and the normal coordinated electrical functioning of the whole heart is what makes it readily detectable in surface electrocardiograms. The propagation of activity and the coordination of the electromechanical functioning of the heart also depends on electrical coupling between cells, which is mediated by gap junctions.

The heart cells that are directly involved in the dynamics of its electrical activity include pacemaker and nonpacemaker cells. The pacemaker cells generate spontaneous action potentials and are characterized by a slow rate of depolarization. These cells are found in sinoatrial and atrioventricular nodes and initiate the propagation of electrical activity throughout the heart. For a detailed description of the genesis of cell electrical activity refer to appendix A.
The non-pacemaker cells, involved in the propagation of electrical activity, such as atrial myocytes, ventricular myocytes and Purkinje cells, have a specific form of action potential which is characterized by five main phases.
Myocardial electrical activity is initiated in the pacemaker cells in the sinoatrial node and then propagated through the atria to the atrioventricular node. Following a brief pause in

the atrioventricular node, excitation spreads in the conducting Purkinje fibers to the apex of the heart and into the working ventricular myocardium.
Within cells in each of these specialized regions, excitation results in action potential generation, followed by relaxation and a period of refractoriness until the next impulse is generated and propagated (figure 1.1). The observed heterogeneity in action potential waveforms in different cell types reflects differences in ion channel expression levels.
The depolarization and repolarization deflections in transmembrane voltage conducing to the generation of action potentials in any cell, including cardiac cells, are a result of ionic currents that flow through specialized, pore forming membrane proteins, called ions channels. Ion channels can select ions by size or by charge and their operating status, open, closed or inactive can be controlled by the potential difference across the membrane, by mechanical stimulation, by neurotransmitters or other molecules.

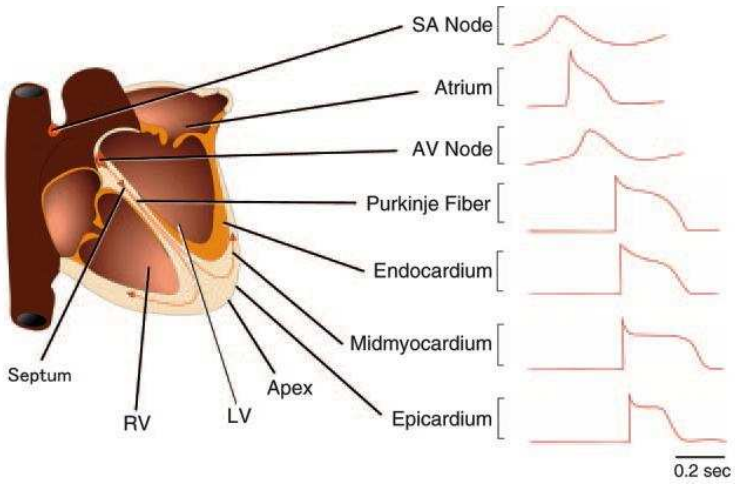

Figure 1.1: Cardiac Action Potential. [3]

The phases of the cardiac action potential are designated by the numbers 0 through 4, beginning with initial depolarization (phase 0) to the return to the resting state (phase 4).
The cellular resting potential is set mainly by the resting potassium K^+ conductance, which is normally large in non-nodal tissue because of a high resting permeability through inward-rectifier current (I_{K1}) channels. Being depolarized to the threshold voltage of about -70mV, cardiac cells show a very rapid depolarization caused by the opening of fast sodium channels Na^+ (phase 0).
This phase quickly increases the membrane potential to positive values where the Na^+ channels become inactivated and the dynamics of the membrane changes to an initial repolarization (phase 1) due to K^+ egress through a rapidly activating and inactivating

transient outward current (I_{to}) K^+ channels. This transient repolarization or "notch", which can be quite prominent in Purkinje and ventricular cells, influences the height and duration of the action potential plateau.

The plateau of cardiac action potential (phase 2) is the result of balanced dynamics between the inward calcium L-type Ca^{2+} current (I_{CaL}) and the outward K^+ current coming through the slow delayed rectifier potassium channels. The plateau in a crucial phase of the cardiac action potential for it directly influences the duration of the action potential and consequently the length of the tissue refractory period.

The influx of Ca^{2+} through L-type Cav channels during the phase 2 plateau is the main trigger for excitation-contraction coupling in the working myocardium. During this phase there is progressive time-dependent activation of delayed-rectifier currents, particularly the rapid delayed-rectifier I_{Ks} which finally terminate the action potential with appropriate delay by producing rapid phase 3 repolarization. The cellular resting potential (phase 4) is again reached, thus concluding the cardiac cycle (figure 1.2).

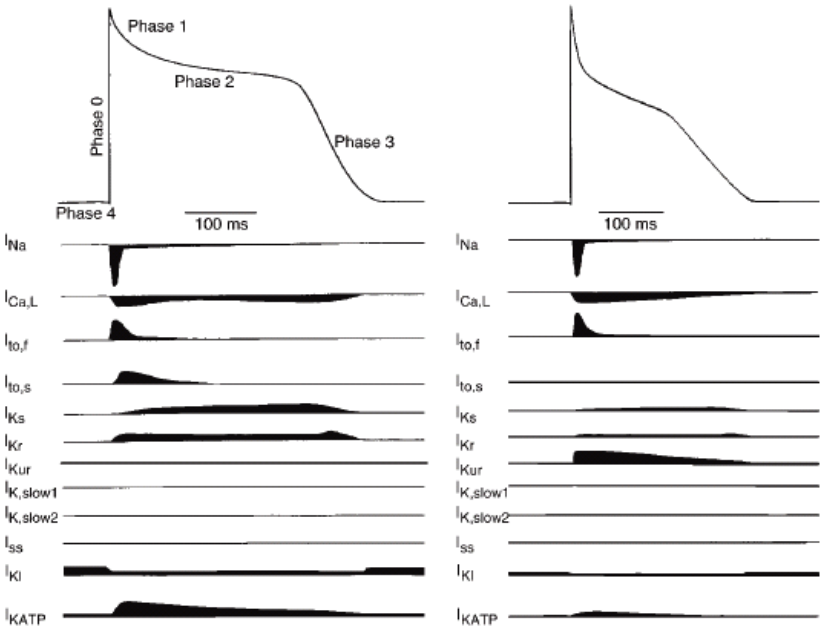

Figure 1.2: Cardiac Action Potential Currents. [3]

In addition to the above mentioned ion channel currents there are multiple types of voltagegated K^+ (Kv) currents, as well as non-voltage-gated, inwardly rectifying K^+ (Kir) currents that contribute to myocardial action potential repolarization. At least two types of transient outward currents, $I_{to,f}$ and $I_{to,s}$, and several components of delayed rectification, including I_{Kr} [IK(rapid)], I_{Ks} [IK(slow)], and I_{Kur} [IK(ultrarapid)], have been distinguished. The relative Kv channel expression levels vary in cardiac cells in

different regions (i.e., atria, ventricles) of the heart, and this heterogeneity contributes importantly to the observed regional differences in action potential waveforms observed in figure 1.1.

The differences in expression and/or properties of ion channels and consequent diversity in action potential waveforms throughout the heart contribute to the normal unidirectional propagation of excitation through the myocardium and to the generation of normal cardiac rhythms [3]. Changes in the properties or the functional expression of myocardial ion channels, resulting from inherited mutations in the genes encoding these channels or from myocardial disease, can lead to changes in action potential waveforms, synchronization, and/or propagation, thereby predisposing the heart to potentially life-threatening arrhythmias. These alterations appear in many instances to be part of the homeostatic adaptive response to a primary abnormality, but often result in secondary cardiac dysfunction, including excessively rapid cardiac rhythms called tachyarrhythmias.
For example, changes in the properties or the functional expression of Kv channels, as occurs in a variety of myocardial diseases, can, therefore, have dramatic effects on action potential waveforms, propagation, and rhythmicity. The densities and the functional properties of myocardial Nav, Cav, Kv, and Kir currents also change in a number of acquired myocardial disease states [4].

In AF the normal ionic currents that characterize the atrial action potential are disturbed by the arrhythmia and this fact might be determinant for the perpetuation of the disease.

1.2 Pathophysiology of AF

During AF a formed atrial contraction does not exist and so one of its hallmark signs is the absence of normal P waves in the electrocardiogram.
During AF, re-entry conduction occurs throughout the atria and ectopic pacemakers may be present. The conduction intermittently passes through the AV node into the ventricles, causing the QRS complexes to occur at irregular intervals. This leads to an irregular heart rhythm with ventricular contraction occurring at rates higher than 100 beats per minute in most patients. This situation is called rapid or uncontrolled ventricular response. Various diseases that cause an alteration in atrial chamber pressures are associated with this dysrhythmia. The resultant dilation facilitates disorganized atrial conduction that leaves the normal conduction pathway intermittently and circles back into the conduction pathway. This conduction is called a re-entry circuit. Re-entry circuits and ectopic foci

represent the underlying conduction abnormalities of atrial fibrillation [5].

Atrial fibrillation may be classified on the basis of the frequency of episodes and the ability of an episode to convert back to sinus rhythm. If a patient has two or more episodes, AF is considered to be recurrent. Recurrent AF may be paroxysmal or persistent. If AF terminates spontaneously it is designated as paroxysmal, and if is sustained is designated as persistent. Persistent AF may present either as the first manifestation of the arrhythmia or as the culmination of recurrent episodes of paroxysmal AF. The category of persistent AF also includes permanent AF, which refers to long-standing (generally $>$1 year) AF for which cardioversion was not indicated or attempted.
Some patients with AF have no predisposing factor or identifiable cardiac lesions. The condition in these patients is classified as “lone” or “idiopathic” atrial fibrillation. Lone atrial fibrillation can be either paroxysmal or persistent, and is present in between 3% and 11% of all patients with AF.

For many years the electrophysiological mechanism of atrial fibrillation was thought to involve several coexisting re-entrant wavefronts or wavelets continuously sweeping around the atria, repeatedly encountering excitable myocardium. This is called the ”multiple wavelet” model and suggested that AF is sustained by this multitude of simultaneous wavelets wandering randomly throughout the atria. The phenomenon of re-entry is a conduction anomaly promoted by decreased atrial refractory periods, slowed conduction and an increased mass of cardiac tissue.
Recent insights about the factors involved in the initiation and maintenance of AF suggest a more complex mechanism, including a set of possible triggers that induce AF and the substrate that has the ability to sustain it.
Triggers include sympathetic or parasympathetic stimulation [6], bradycardia, atrial premature beats or tachycardia, accessory atrioventricular pathways, and acute atrial stretch. Recently identified as triggers are ectopic foci occurring in “sleeves” of atrial tissue within the pulmonary veins or vena caval junctions. These regions under normal circumstances manifest synchronous electrical activity but develop delayed afterdepolarizations and triggered activity on rapid pacing or acute stretch [7]. Triggers propagating into atrial myocardium may initiate reentering wavelets if the wavelength is sufficiently short. Wavelength shortening can occur even in normal atria if the effective refractory period or conduction velocity is decreased. These triggers may also fire repetitively and contribute to the maintenance of AF, essentially becoming “drivers” of AF [8].
Initiation and maintenance of AF may depend on uninterrupted periodic activity of a few

discrete reentrant sources localized to the left atrium, emanating from such sources to propagate through both atria and interact with anatomical and/or functional obstacles, leading to fragmentation and wavelet formation.

Having been initiated, AF may be brief. A variety of factors may act as perpetuators, ensuring the persistence of AF for longer periods. One is persistence of the triggers and initiators that induce AF, but at some point, AF persists even in their absence. Persistence here may result from electrical and structural changes, characterized by atrial dilatation and shortening of the atrial efective refractory period. This combination, along with other changes, likely facilitates the appearance of multiple reentrant wavelets (a final common pathway for AF) [9].

The longer AF persists, the more difficult it is to restore sinus rhythm and prevent recurrence. This is because AF induces a series of changes within the tissue. The process by which these alterations in electrophysiological, mechanical and structural properties of the tissue take place, caused by the arrhythmia itself is termed “atrial remodelling in AF”. It encompasses a variety of changes including alterations in sarcolemmal ion channel gene expression, cellular size and content, in addition to changes in connexins that couple cells electrically. The net effect of these modifications is to decrease the atrial refractory period and possibly interfere with atrial conduction in a spatially heterogeneous way, i.e., the magnitude of the changes varies in different locations, increasing electrical heterogeneity and thus promoting fibrillation, thereby providing a substrate for multicircuit re-entry and facilitating reinitiation of AF, should it end. Moreover, sustained AF causes important reductions in cellular contractility, resulting in a tachycardia-induced atrial cardiomyopathy that may be responsible for delayed thromboembolic events as contractility recovers after cardioversion.
A rapid heart rate like in AF reduces the diastolic filling interval, and the additional loss of the sequential atrioventricular contraction mechanism in atrial fibrillation may lead to a dramatic reduction in cardiac output and to other haemodynamic disturbances.

1.3 Atrial Fibrillation and Autonomic Nervous System

While most research has been focused on the molecular and physiological mechanisms, the autonomic nervous system has not been consistently viewed as a critical part of the puzzle in the approach to patients with AF. It is generally accepted that changes in autonomic outflow are present before, during, and after episodes of AF; however, the role

of the autonomic nervous system (ANS) variations in the initiation, maintenance, and termination of AF remains unclear and occasionally a source of controversy [10].

The ANS is a part of the peripheral nervous system that functions to regulate the basic visceral processes needed for the maintenance of normal bodily functions and homeostasis. It has an important function in maintaining the internal environment of the human body in a steady state. This role is vital in returning the body to a homeostatic state after trauma and also to cope with and adapt to everyday changes.
The ANS consists of two major divisions: the sympathetic nervous system and the parasympathetic nervous system. These often function in antagonistic ways. However it is important to remember that they all form part of an integrated whole and that both the sympathetic and the parasympathetic nervous system are operating continuously along with the rest of the nervous system. In general, the autonomic nervous system controls homeostasis, which is the constancy of the content of tissues in gases, ions, and nutrients. A more complete description of the anatomy and physiology of the autonomic nervous system is provided in appendix B.

1.3.1 Autonomic cardiovascular control

An individual's heart rate is constantly changing is response to the metabolic requirements of the body or changes in the environment that cause or alleviate stress. Various intrinsic, neural, and hormonal factors act to influence the rhythm control and impulse conduction within the heart. The rhythmic control of the cardiac cycle and its accompanying heartbeat relies on the regulation of impulses generated and conducted within the heart. The sympathetic and parasympathetic divisions of the autonomic system regulate heart rhythm by affecting the same intrinsic impulse conducting mechanisms that lie within the heart in opposing ways.
Extrinsic control of the heart rate and rhythm is achieved via ANS impulses (regulated by the medulla oblongata) and specific hormones that alter the contractile and or conductive properties of heart muscle. In very simple terms, the sympathetic division of the ANS works, via the cervical sympathetic chain ganglia, to increase the heart rhythm and contractibility in situations of stress or increased metabolic demand. In contrast the parasympathetic division of the ANS works, via the vagal nerve, to decrease heart rhythm and contractibility in situations of decreased metabolic demand. Sympathetic stimulation also increases the conduction velocity of cardiac muscle fibers. Parasympathetic stimulation decreases conduction velocity. The regulation in impulse conduction results

from the fact that parasympathetic fibers utilize acetylcholine as a neurotransmitter hormone that alters the transmission of the action potential by altering membrane permeability to specific ions (e.g., potassium ions K^+). In contrast, sympathetic postganglionic neurons secrete the neurotransmitter norepinephrine that alters membrane permeability to sodium (Na^+) and calcium ions (Ca^{2+}).

Cholinergic mechanisms have long been known to play an important role in the occurrence and maintenance of AF [11]. Vagal-nerve stimulation decreases the atrial refractory period in a spatially heterogeneous way. The vagally mediated decrease in refractory period reduces the wavelength and the size of potential reentry circuits, resulting in multiple-circuit reentry, a final common pathway for AF. Increases in refractoriness heterogeneity appear to be particularly important in the AF-promoting effects of vagal stimulation. The atrial repolarization heterogeneity-promoting effects of vagal stimulation may be caused by patchy distribution of vagal nerve terminals and acetylcholine receptors. This action appears to depend both on refractoriness shortening at the site of premature impulse generation and on heterogeneous effects that cause the premature wave front to block in a region with a lesser degree of refractoriness abbreviation.

Whereas the role of vagal-nerve activation in promoting experimental and clinical AF is progressively more established, the role of sympathetic activation is much more cloudy. Sympathetic-nerve stimulation abbreviates atrial refractoriness, but, for a comparable degree of refractoriness and wavelength abbreviation, bilateral sympathetic outflow stimulation has a much smaller AF-promoting action than bilateral cervical vagal-nerve stimulation. This difference may be caused by a much more spatially heterogeneous effect of vagal stimulation. Nonetheless, sympathetic activation may be important in some types of AF. Research to elucidate this matter is on course using *in vivo* animal models of FA.

1.4 Ionic remodelling in Atrial Fibrillation

Whatever the initial cause of AF or the determinants for its recurrence, electrical remodelling is likely to be a final common pathway that ultimately supervenes. Recent advances in understanding ion channel function, regulation, and remodelling at the molecular level have allowed for a much more detailed appreciation of the basic determinants of AF.

The recognition that AF alters atrial electrophysiological properties (electrical remodelling), promoting AF induction and maintenance, was an important advance in AF

pathophysiology [12].

As stated before, AF-promoting effect of AF is associated with a progressive decrease in atrial effective refractory period (ERP) and in the AF cycle length, an indicator of ERP during AF. Similar changes are observed after either electrically maintained AF or rapid atrial pacing in experimental models [13]. AF induces electrical remodelling primarily by virtue of a very rapid atrial rate. Whether AF can produce additional forms of structural or autonomic remodelling, particularly when the arrhythmia remains sustained for prolonged periods, remains uncertain.

The evolving information regarding atrial tachycardia-induced remodelling (ATR) has fundamental implications regarding the mechanisms of AF. Since all cases of AF involve very rapid atrial activation, tachycardia-induced remodelling will inevitably follow, irrespective of the mechanisms initially involved. Thus, even if AF begins as a result of other mechanisms, such as single reentrant circuits (mother waves) with fibrillatory conduction or rapid ectopic activity, tachycardia remodelling will act as a final common pathway to reduce the wavelength in a heterogeneous fashion and promote multiple-circuit reentry. The molecular basis of the atrial electrophysiological remodelling induced by atrial tachycardia is beginning to be unraveled.

All these changes that occur in the heart tissue as a response to AF and in an analogous way in ATR are thought to be caused, initially by functional adaptation of the cardiac ion channels, and latter by the regulation of their genetic expression levels. Of course there can be numerous possible (transcriptional, translational, and posttranslational) mechanisms that could be involved in regulating the functional expression and the properties of these channels.

The prominent changes in atrial refractoriness caused by AF (and atrial tachycardias in general) point to important alterations in the atrial action potential and particularly action potential duration (APD), the principle cellular determinant of the refractory period. These alterations include a loss of the plateau and decreased APD, as well as increased APD heterogeneity.

These action potential alterations were subsequently observed to develop progressively in dogs as a result of pacing-induced atrial tachycardia (400 bpm). Furthermore, pacing-induced APD alterations in isolated cells correspond closely to refractory period changes in vivo indicating that cellular action potential modifications likely account for the refractory period changes that promote AF [14].

In addition to alterations in the steady-state values of APD at different frequencies, AF

also affects the dynamics of APD alterations associated with premature beats and with abrupt rate change. The modified APD dynamics produced by atrial tachycardia are related to important alterations in Ca^{2+} handling, which likely contribute to the transient atrial contractile dysfunction observed after cardioversion of AF [15].

In addition to decreasing atrial ERP, long-term atrial tachycardia appears to slow intra atrial conduction, thus tending to decrease the wavelength for reentry. Furthermore, changes induced by remodelling are spatially heterogeneous, increasing the heterogeneity in atrial refractory properties [16]. The combination of decreased wavelength and increased heterogeneity would be expected to promote multiple circuit reentry [17].

Although results are not always confirmed by different available studies, using different animal models, most agree upon that long term ATR, as a simulation of AF remodelling, abbreviates atrial refractoriness by decreasing APD [13, 14, 18, 19, 20]. The timescale of these changes is not yet well defined but most available studies converge to approximately the same results after long periods of rapid pacing. This happens primarily by I_{CaL} downregulation but also via increased inward rectifier K^+ currents such as the background current I_{K1} and a constitutively active form of acetylcholine-dependent K^+ current ($I_{KACh,c}$), which is closely related with autonomic vagal activation. In addition, ATR impairs atrial contractility, principally by causing Ca^{2+} handling abnormalities, which causes atrial dilation that further promotes reentry.

The abrupt 8-fold increase in atrial rate with the onset of AF substantially increases Ca^{2+} loading. Atrial cardiomyocytes respond by reducing Ca^{2+} influx via I_{CaL} to prevent potentially cytotoxic Ca^{2+} overload, but reduced I_{CaL} decreases APD and wavelength, which favors AF perpetuation. Initially, rapid APD shortening occurs because of functional I_{CaL} inactivation. Sustained AF causes more persistent I_{CaL} decreases, predominantly via downregulation of I_{CaL} poreforming-subunit mRNA.

The cardiomyocyte resting membrane potential is set by background K^+ conductances, primarily inward rectifiers, and becomes more negative in AF. The main background conductance that controls atrial resting potential is designated I_{K1} and is formed by Kir2 family subunits, especially Kir2.1. AF increases expression levels of Kir2.1 mRNA and protein, which enlarges I_{K1}. The inward rectifier K^+ current I_{KACh} mediates cardiac vagal effects: Acetylcholine released from vagal nerve endings activates I_{KACh}, which causes APD abbreviation and cell membrane hyperpolarization. Increased vagal activity strongly promotes AF by stabilizing atrial reentrant rotors, and clinical AF often begins under vagotonic conditions. $I_{KACh,c}$ blockade suppresses ATR induced APD abbreviation and

AF promotion, which indicates that $I_{KACh,c}$ plays an important role in arrhythmogenesis.

The transient outward K^+ current (I_{to}) is consistently decreased in ATR. The functional consequences of I_{to} downregulation are unclear; however, I_{to} activates quickly and produces an outward-current component that can oppose inward Na^+ current during the action potential upstroke, so I_{to} downregulation may facilitate wave propagation by indirectly increasing action potential amplitude. Decreased I_{to} parallels reductions in both mRNA and protein expression of its pore forming Kv4.3 subunit. Atrial tachycardia also appears to reduce I_{Na}, possibly accounting for conduction slowing after prolonged periods of atrial tachycardia. Reported AF associated changes in the ultrarapid delayed rectifier I_{Kur}, mediated by the Kv1.5 channel have been inconsistent. The role of I_{Kur} in atrial repolarization depends strongly on action potential morphology and is increased with the short duration, triangular action potentials that occur in AF.

Decreased expression of connexins has also been reported as a consequence of rapid atrial pacing, possibly contributing to a slower conduction velocity of cardiac action potential throughout the heart. In addition to the expression changes, connexins can also have a deficient distribution across the cardiomyocite plasma membrane. In this case the lateralization of connexins further contributes to the decreased conduction velocity of the action potential [21].

Studies of ionic currents in patients with AF are complicated by the potential effects of concurrent cardiac disease and drug therapy; however, the limited data available are in general agreement with results in animal studies.

Patients with persistent AF have significant decreases (average decrease ranging from 49 to 60%) in mRNA encoding L-type Ca^{2+} channel a1c subunits. Expression levels of Na^+-Ca^{2+} exchanger, mRNA were unaltered but a decrease in sarcoplasmic-reticulum Ca^{2+} ATPase mRNA of variable magnitude has been noted. L-type Ca^{2+} channel protein levels were also found to be reduced.

When the ionic current alterations reported in atrial myocytes from patients with AF are incorporated into a mathematical representation of the human atrial action potential, based on detailed formulations of directly measured ionic currents [22], the results resemble recorded action potentials closely. Evaluation of the contributions of individual ionic current alterations to action potential alterations in the mathematical model suggests that reductions in I_{CaL} account for most of the action potential abnormality associated with AF in humans.

Recently several mathematical models of cardiac properties have been published, con-

firming some of the ionic parameters underlying triggered activity, fibrillatory conduction and reentry circuits, thus confirming the experimental data [23, 24, 25].

The ionic changes seen in cells from patients with chronic AF are not observed in patients with sinus rhythm and a history of paroxysmal AF, suggesting that they are a result, and not the primary cause, of the arrhythmia. These observations point to decreases in mRNA levels, likely owing to transcriptional downregulation, as the molecular mechanism of tachycardia induced changes in atrial ionic current expression. The signal transduction pathways responsible for changes in mRNA levels induced by atrial tachycardia are currently being investigated [26].

In contrast to the well-defined alterations of cellular and molecular electrophysiology underlying chronic AF, investigated in chronic AF patients and long term animal models of ATR, the initial changes and their time course are currently unknown, although they might be interesting targets for therapeutic interventions. In humans, even AF of several minutes (10 minutes) shortens atrial refractoriness. This shortening is considered to result from physiological responses to the intracellular Ca^{2+} overload by high rate atrial excitation, because this shortening recovered rapidly within several minutes after cessation of AF.

It is well known from in vivo studies that atrial repolarization starts to shorten after very brief periods of AF or rapid atrial pacing and that these changes are associated with an increased inducibility and duration of AF episodes. However the only short term data available on the molecular level showed a transient increase in Kv1.5 (I_{Kur}) mRNA and protein and a reduced mRNA expression of Kv4.2 and Kv4.3 (I_{to}) without changes in protein levels after short periods of RAP in rats [27].

Current	Channel	Genes	Available Results	Effects
all	connexin-40,43	Gja5, Gja1	underexpression/lateralization	decreased conduction velocity
I_{Na}	Nav1.5	Scn5a	underexpression	decreased phase 1 slope
I_{to}	Kv4.2, Kv4.3	Kcnd2, Kcnd3	underexpression	increased action potential amplitude
I_{Kur}	Kv1.5	Kcna5	underexpression/overexpression	prolongated APD_{20}
I_{CaL}	L-type Ca^{2+}	Cacna1	underexpression	decreased plateau/APD
I_{KAch}	Kir3.1, Kir3.2	Kcnj3, Kcnj6	unchanged/underexpression	decreased vagal modulation

Table 1.1: Ion channel remodelling

Results from cardiac ion channels expression studies are sometimes inconsistent when it comes to short periods of RAP, but if a correlation between channel expression levels and ionic currents measured by electrophysiology techniques can be found, in the context of AF, it can provide a useful tool for the understanding of the atrial ionic remodelling

phenomena and for evaluation of its extent in AF patients.

The pathophysiology associated with AF is thus a dynamic function of the underlying cause(s) and the changes resulting from maintenance of the arrhythmia itself.

Chapter 2

Electrocardiogram and Cardiac Potentials

One of the goals of this study is to relate the electrical signals captured from the surface of the heart with changes in expression of ion channels in the cardiac tissue.
The objective described greatly relies on the relative fidelity of the measured electrophysiological signals. The quality and adequacy of the experimental approach used to measure those signals can only be ascertained by comparison with established theories, for although the signals can speak for themselves, one can only be sure of what they say, of what is actually being measured by testing them against the current electrical models of cardiac tissue. For that reason, a comprehensive overview of the methods and theories applied in the measurement of cardiac potential is presented, along with some history on how it all started.

Since the 18th century, when Galvani introduced the concept of “animal electricity”, electric potentials have been observed and recorded in different nerves and muscles, including hearts and isolated preparations of cardiac tissue.
The tracings of the electric activity of the human heart, the electrocardiogram (ECG), were first measured in 1887 by Augustus Waller using a capillary electrometer. Waller found that the cardiac electric generator has a dipolar nature and suggested that the ECG should be measured between the five measurement points formed by the hands, legs, and mouth (a total of 10 bipolar leads).
Not much later, at the beginning of 20th century, the pioneer in modern electrocardiography, Willem Einthoven, developed the first high-quality ECG recorder based on the string galvanometer. Einthoven summarized his fundamental results in ECG research

in 1908 and 1913, and received the Nobel Prize for his work in 1924. The discovery of the string galvanometer by Einthoven established, in the beginning of this century, electrocardiography as a viable clinical application.

In these first experiments regarding the electrical activity of the heart, it was observed that, when measuring the potential difference between a small macerated cardiac area and an intact one, the injured region showed negativity in relation to the intact one (figure 2.1). The potential observed was named “injury potential”. The existence of a cellular potential was inferred by measuring this injury potential. The probable explanation for the existence of this potential is that injury destroys the selective permeability of the cellular membrane, reducing the membrane’s electrical resistance, allowing that an electrode placed in the injured region contacts the cellular cytoplasm through a fluid pathway of relatively low resistance.

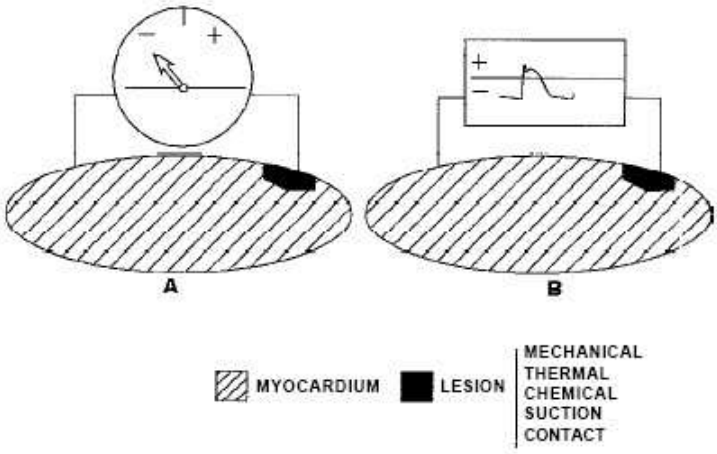

Figure 2.1: A) Sketch of the injury potential; B) Sketch of the action potential obtained through the injury technique. [28]

This technique was the first to produce monophasic recording of the heart’s activity, as opposed to the multiphasic deflections observed placing electrodes in intact heart tissue, and it was very important in the discovery of several electrophysiological properties of excitable tissue including the action potential, for it closely resembles the dynamics of the cell’s actual transmembrane potential.

This technique has a major drawback, which is the need to inflict some kind of damage to the heart muscle in order to record a signal. This quite significant inconvenience limited the clinical application of the technique that remained deterred in favor of less damaging methods like the electrograms.

Electrograms or electrocardiograms are time-dependent signals that are recorded from the active heart using a specific electrode configuration. When two electrodes are gently placed on the heart surface, the recorded signal is called a bipolar electrogram.
The latu sensu electrograms, which include the surface electrocardiogram (ECG) in all its variations and the intracavitary electrographic recordings, provide a distance view of the cardiac electric phenomena, because they represent the summation of the cellular electric activity of a bigger or smaller cardiac area, depending on the technique used. What is actually obtained is the picture of action potentials distorted by their algebraic sum, dispersed in time and space and modified by the capacitances and resistances found in the way (figure 2.2).

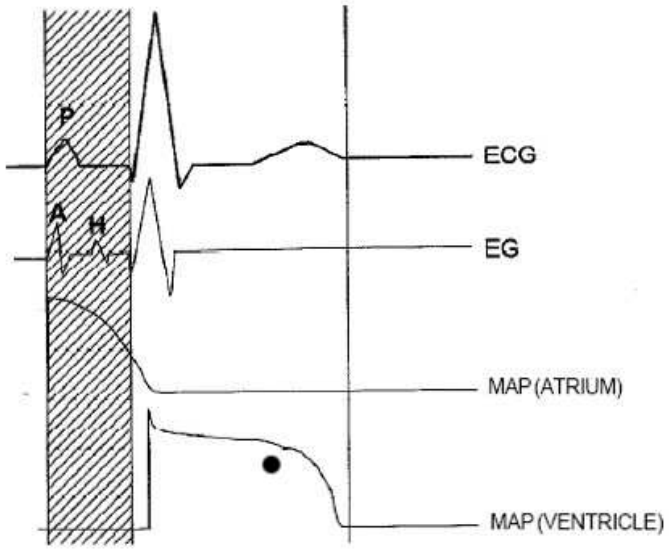

Figure 2.2: Electrocardiogram, Electrogram and MAP. [28]

However, in regard to the moment of the occurrence of electrical events of the cardiac cycle, electrograms provide very precise and useful data, hence its fundamental importance in the diagnosis of arrhythmias. But in many situations, it is important to know in detail the entire temporal extension of cellular action potential. Therefore an indirect method is required; one that does not damage to the cells like the electrogram, but at same time delivers the increased fidelity of the injury potential.
Fulfilling this demand Jochim et al [29] published in 1935 the first method for nontraumatic monophasic action potential recording (MAP). These authors demonstrated that MAPs can be obtained by simply pressing an electrode against the epicardium while another electrode merely touched the nearby epicardium. They also showed that the MAP is positive with respect to zero if the pressure electrode is the active electrode (connected

to the positive amplifier input).

The essential aspect of Jochim's method is the mechanical pressure that when applied on one of the electrodes permanently depolarizes the cardiac tissue beneath it.

This new method of recording the electrical activity of the heart muscle produces measures with great fidelity, and that closely resemble the transmembrane action potential [30], without the drawbacks of the injury potential method (figure 2.3). This fact allowed for the adaptation of this technique to clinical practice and in the study of several cardiac arrhythmias [31, 32].

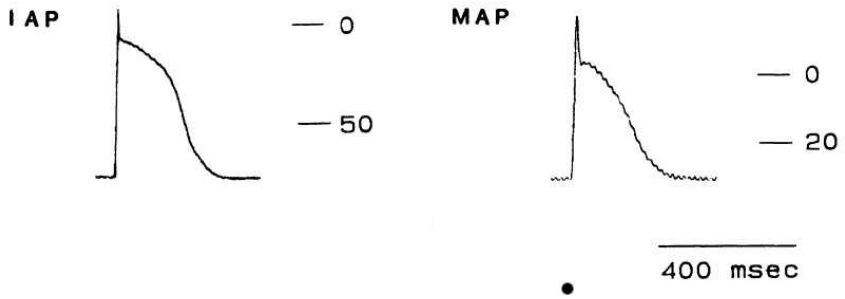

Figure 2.3: Intracellular action potential and Monophasic action potential. [30]

The exact mechanisms by which the MAP potentials are recorded and their origin is still matter of active debate [33, 34]. Several methods or electrode set ups have been proposed to measure MAPs and different models that try to explain the mechanisms that originate the measured potentials have been suggested. Although a definitive theory is not currently available, the "volume conductor" hypothesis devised by Franz [35] is the most experimented and accredited theory.

The volume conductor hypothesis suggests that the MAP measured by the contact electrode method results from a current source, with cardiac cells acting as individual electromotive generators organized more or less in series.

The pressure exerted focally by the electrode, against the myocardium depolarizes the group of cells subjacent to the electrode to a level that is estimated at -30 to -20 mV with respect to the diastolic extracellular reference potential. Because sodium channels remain inactivated at these voltage levels, these cells are unexcitable and thus unable to participate in the periodic depolarizations and repolarizations that occur in the adjacent (normal) myocardium. The group of cells depolarized by the contact electrode provide a "frozen" potential, which contrasts with the time-varying potential in the unaffected adjacent cells. Assuming preserved electrical coupling, this causes a time-varying electrical gradient between the depolarized (inexcitable) cells subjacent to the electrode

and the adjacent (excitable) cells. This electrical gradient produces current flow across the boundary between these two states. During electrical diastole, this gradient results in a source current emerging from the normal cells and a sink current descending into the depolarized cells subjacent to the MAP electrode. The sink current produces a negative electrical field that is proportional to the strength of current flow, which depends on the potential gradient and the number of cells that contribute to the interface between the subjacent depolarized and the adjacent nondepolarized cells. During electrical systole, the normal cells adjacent to the MAP electrode undergo complete depolarization, which overshoots the zero potential by some 30 mV, whereas the already depolarized and therefore refractory cells subjacent to the MAP electrode cannot further depolarize and maintain their potential at the former reference level. As a result, the former current sink reverses to a current source, producing an electrical field of opposite polarity. The process is illustrated in figure 2.4. According to this hypothesis, the MAP recording reflects the voltage time course of the normal cells that bound the surface of the volume of cells depolarized by the contact pressure. Thus, both the depolarized (electrically frozen) cells and the active cells of the neighboring myocardium contribute to the genesis of the boundary current that produces the MAP field potential; one cannot exist without the other.

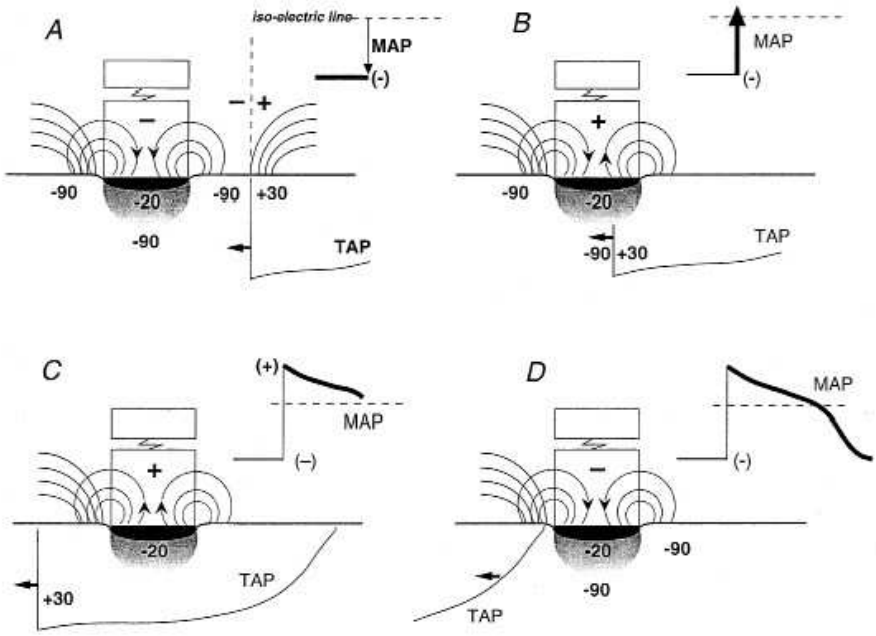

Figure 2.4: Origin of the MAP. [37]

This view was not shared by Schutz [36], that defended a theory based on a voltage source with all electromotive generators in parallel. Schutz related the MAP amplitude with the intracellular and extracellular resistances, and this relation can be observed experimentally. But he also assumed that in order to record a MAP an "electrical seal" between the active electrode and the surrounding medium was crucial, condition that was later found to be unnecessary by experiments where intracavitary MAP recording were performed using contact electrodes.

According to the Franz's model [37, 38], the MAP originates from cells in the immediate vicinity of the electrode that causes persistent depolarization. Therefore to obtain an upright MAP signal, the MAP-exploring electrode should be connected to the positive input of the amplifier and the reference electrode to the negative input, as initially stated by Jochim. This matter of which of the electrodes is the measuring electrode is still in active debate with authors like Kondo [39, 40], counteracting the traditional view and stating that the recording electrode is not the pressure electrode, but the contact one.

Controversy aside, the applicability of the volume conductor hypothesis, for the experimental conditions used will be assumed, since the measured signals fall into the predictions of this hypothesis. Also, only this model explains the measurement of MAPs using only one pressure electrode over the myocardium referenced to a distant electrode, in what is called the unipolar MAP [41]. Concurrent theories that consider the pressure electrode to be the reference one cannot explain the results obtain using this kind of measurement arrangement. That reason alone suffices in deeming them unfit, at least to model the particular conditions of the experiments carried.

Considering the experimental conditions associated with the measurement of *in vivo* atrial MAPs in the anesthetized rat, it is easy to notice that the minute scale of the preparation does not easily allow the placement of two, closely placed electrodes in the surface of the beating atrial myocardium. For this reason the MAP-exploring electrode was coupled with a remote electrode placed in the thoracic wall. With this set up, often referred to as unipolar MAP (figure 2.5), one still obtains a monophasic potential, but it also contains far-field potentials. The extent to which these far-field potentials contribute to the local MAP signal is often unpredictable, but generally there is a decrease in upstroke velocity, unclear phase two and relatively unstable baseline when compared to the close bipolar MAP.

In the clinical environment MAP recording can be measured using a commercial endocavitary MAP recording catheter. This is a minimally invasive procedure, especially

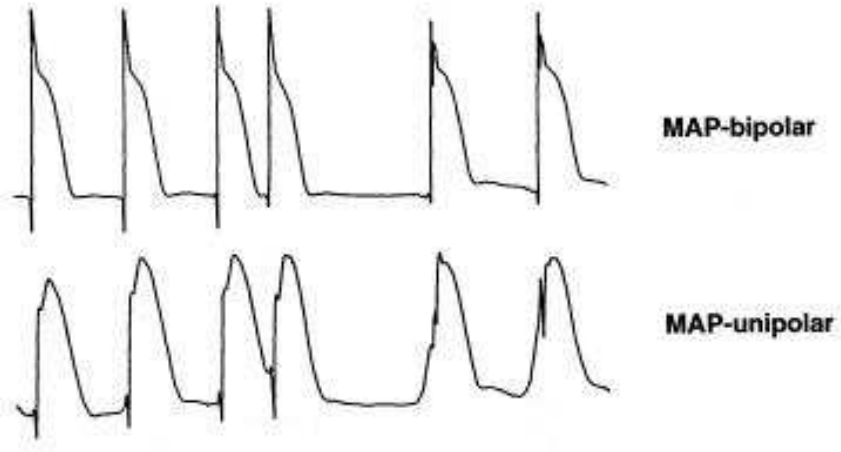

Figure 2.5: Unipolar MAP. [37]

when compared to sampling of cardiac tissue for gene expression analysis.

Chapter 3

Materials and Methods

3.1 Animal Experimental Model

In the field of supraventricular and ventricular arrhythmias there as been a strong interaction between experimental and clinical studies and there can be no doubt that the various animal models have been instrumental in understanding the mechanisms of clinical arrhythmias and in establishing different forms of therapy. Clearly, an animal cannot be transformed into a human patient, but despite differences between species and differences in arrhythmogenic factors in animal models and humans, the similarity between arrhythmia mechanisms in experimental models and patients far outweigh these differences.

Some crucial observations on the characteristics of atrial fibrillation were made on animal models of atrial fibrillation simulated through the use of rapid atrial stimulation, normally designated rapid atrial pacing. These initial findings were made long before technical developments would allow them to be confirmed in clinical studies [42].

In the reported study experiments were performed in 65 Wistar Rats, aged more than 10 weeks, anesthetized with sodium pentobarbitone (Pentothal, 60 mg/kg, intra peritoneal) supplemented as necessary.

The femoral artery and vein were cannulated for monitoring arterial blood pressure (Neurolog, Digitimer) and the injection of drugs, respectively. The trachea was cannulated below the larynx and the animal was ventilated with O_2-enriched air applied after induction of neuromuscular blockade with Vecuronium bromide (Norcuron, 4 mg/kg, Intra Venous) using a positive pressure ventilator (Harvard Apparatus Ltd).

An adequate level of anesthesia was maintained by ensuring the absence of a withdrawal

reflex before the neuromuscular blockade. During this blockade, the level of anaesthesia was monitored by recording blood pressure and heart rate. Rectal temperature was maintained at 36.5−38 °C by a servo-controlled heating blanket (Harvard Apparatus Ltd). The electrocardiogram (ECG) was recorded (Neurolog) from subcutaneous electrodes placed in the limb's origin. Heart rate was derived from the ECG.

A mid-line thoracic incision was made to expose the heart in order to record and stimulate the atria. Two recording electrodes were placed in the right and, whenever possible, in the left atrial surface respectively and a concentric bipolar stimulating electrode was placed in the right atrial surface in order to perform rapid atrial pacing. Stimulation at a frequency of 50 Hz or 3000 bpm was performed for periods of 30 minutes, 2 hours and 4 hours, using 1ms rectangular pulses, with the use of a programmable stimulator and a constant current source (Master-8, Iso-Flex).

At the end of the experiment, the animals were killed with an overdose of anesthetic and samples of the right and left atria were collected for RNA quantification.

The animals were classified into seven groups according to the recording and pacing duration. In thirty animals only atrial recordings were perform, in thirty animals atrial recordings and atrial pacing were perform and in five animals only the surgical procedures were perform.

Duration	Atrial Pacing	Control Surgery
0		5
30 minutes	10	10
2 hours	10	10
4 hours	10	10

Table 3.1: Number of animals used per experimental condition

3.2 Gene Expression Analysis

Messenger RNA quantification was made for a set of ten genes, which code for membrane proteins involved in the generation and conduction of action potentials throughout the cardiac tissue, including connexins and ion channels. The measured quantities of mRNA are not a sole indication of genetic expression, for there are other post-transcription mechanisms that influence the amount of functional protein produced. Even so, for simplicity, the terms expression, underexpression and overexpression will be used to refer to measured mRNA levels.

Connexins are proteins that connect cardiac myocytes allowing for the rapid transmission of action potential from one cell to the following one. Normally these proteins are placed at the extremities of long cardiac cells, and their relative number can influence the conduction velocity of the cardiac action potential throughout the myocardium. Genes coding for two types of connexins where analysed, Gja5 for the connexin-40 and Gja1 for the connexin-43.

Expression analysis for gene Scn5a coding for an I_{Na} sodium channel was also performed. This channel is crucial for the initial depolarization of the action potential (phase 1) and changes in its expression can influence the amplitude and speed of the upslope of the atrial activation.

The Kcnd2 and Kcnd3 were also analysed. These are genes that code for voltage-gated, Kv4 family, potassium channel involved in the transitory, phase 2, repolarization. The relative expression of this channel can also influence the amplitude and duration of the cardiac action potential.

The Kcna5 gene as also analysed, it codes for the Kv1.5 rapid delayed rectifier potassium channel, which influences the I_{Kur} repolarization current that affects the duration of the phase 3 plateau of the cardiac action potential. Pharmacological blockage of this channel as proven to increase the duration of the cardiac action potential's plateau, and consequently it's duration.

Another analysed gene was Cacna1, it is the gene coding for the L-type Ca^{2+} channel, which greatly influences the activation-contraction coupling, and the plateau of the cardiac action potential. The I_{CaL} current partially determines the action potential duration and refractory period of the cardiac tissue.

Next the Kcnj3 and Kcnj6 genes that code for a Kir3 family, inward rectifier, K^+ channel. This channel is activated by Acetylcholine and the respective current I_{KACh} has a determinant effect on the control of heart rate by the autonomic nervous system, namely the parasympathetic division mediated by the vagus nerve. Increased I_{KACh} hyperpolarizes the cell, making it more difficult to reach the threshold action potential voltage.

Finally the expression of gene Cftr coding for a Cl^- channel was also analysed. The role of this specific I_{Cl} current in the cardiac action potential is not clear yet, but it is thought to be activated under stress conditions contributing to the shortening of the action potential. Its influence in the ionic atrial remodelling was also investigated.

3.2.1 Sample Preparation

After harvesting, the ∼30 mg of tissue samples were placed in about 10 volumes of RNAlater, RNA Stabilization Reagent (Qiagen, Valencia, USA) and kept at 4 ^{o}C overnight. After that period samples were frozen at -20 ^{o}C for storage.
The procedures of gene expression analysis described below were conducted in the Instituto Nacional Dr. Ricardo Jorge by Dr. João Paulo Gomes and his research team.

3.2.2 RNA Extraction

Total RNA from each sample was extracted using the RNeasy Fibrous Tissue Mini Kit (Qiagen) according to manufacture's instructions. In order to remove residual DNA, an on-column DNase digestion using 30 Kunitz U of RNase-free DNase (Qiagen) was performed. This step was performed twice to ensure complete DNA removal. RNA was eluted by adding 50 μl of RNase-free water and quantified at A260. The RNA extraction method yielded up to 30 μg from each T25 flask, and purity was verified in the real time-PCR assays as described below. All RNA samples were stored at 80 ^{o}C in RNase-free tubes.

3.2.3 Reverse transcription reaction (RT)

RNA samples were pooled in groups of five (using 400 ng of each individual sample), representing identical experimental conditions. The same procedure was applied for control samples. cDNA of each pooled group was generated from 400 ng of RNA using TaqMan RT Reagents (Applied Biosystems, Foster City, CA, USA). The reaction mix included 5.5 mM $MgCl_2$, 500 μM dNTPs, 2.5 μM random hexamers, 1X RT Buffer, 0.4 U/μl RNase Inhibitor and 1.25 U/μl MultiScribe RT in a final volume of 100 μl. The RT conditions were 10 min at 25 ^{o}C, 30 min at 48 ^{o}C and 5 min at 95 ^{o}C. The cDNA concentration was measured using the A260 value. Each RT reaction resulted in up to 45 μg of cDNA. All cDNA samples were stored in DNase-free tubes at -20 ^{o}C.
We used the two-step RT-PCR assay to avoid differences in RT reaction efficiency for each gene in a sample because 3´ specific primers (used for one-step RT-PCR) may have unequal hybridization efficiency. Using random hexamers, even if some differences in the overall RT efficiency between samples occur, the relative amount of cDNA among the different genes remains the same for the respective sample. This is important for the

relative comparison of transcript amounts in a sample and for the reproducibility of the final real time-PCR.

3.2.4 Real-time Quantitation Assays for Gene Expression

Relative quantitation of gene expression is usually performed using ubiquitously expressed genes that are used as endogenous controls to normalize the quantity of a cDNA target in order to determine differences in the amount of total cDNA in a reaction. Two control genes (B-actin and Arf1) were previously assayed in real time-PCR experiments to evaluate their stability throughout the different time points and experimental conditions, where B-actin showed to be the most stable.
PCR primers were designed using Primer Express software (Applied Biosystems). Also, exhaustive PCR optimization assays were performed for each to ensure the maximum possible efficiency of the real-time PCR with the selected primers. The real-time PCR was run in an ABI PRISM 7000 Sequence Detection System (Applied Biosystems) using SYBR Green technology and 96-microwell optical plates (Applied Biosystems). The PCR reagents consisted of: 1X SYBR Green PCR Master Mix (contains AmpliTaq Gold; Applied Biosystems), 300 nM of each primer and 5 μl of sample cDNA, in a final volume of 50 μl. Each plate contained replicates of the pooled cDNA and different negative controls: no template controls (where all the reaction reagents except for cDNA were used), and RNA samples without RT (RNA from each pooled group was tested for any residual DNA). The thermocycling profile was: 10 min at 94 ^{o}C followed by 40 cycles of 15s at 94 ^{o}C and 1min at 60 ^{o}C. The melting curves of the PCR products were acquired by stepwise increase of the temperature from 60 ^{o}C to 90 ^{o}C.
In order to allow comparison of the expression of all genes at each experimental condition, we used DNA standard curves as chromosomal DNA represents equal amounts of each gene. These DNA standard curves were made using eight serial, two-fold dilutions of DNA (starting at 20 ng of total DNA). Each plate included all pooled groups representing all experimental conditions, and three standard curves (two target genes and one control gene).
For all experiments, the amount of target and control gene was determined from the appropriate standard curve. The quantity of the target gene was divided by the quantity of control gene to obtain a normalized relative value for the target gene. The specificity of the amplified products was verified by analysis of the dissociation curves generated by the ABI 7000 software.

3.3 Data Analysis

In order to extract the subtle variations in atrial MAP a non-linear fit method was used. This method applies a template composed of a set of generalized Gauss functions parameterized by five coefficients, describing relative location, width, amplitude, skew and kurtosis. The fitting is accomplished using an iterative convergence method based on the Levenberg-Marquardt compromise.
The model for each segment of the signal consists of a function composed by the sum of several generalized Gauss functions, expressed by:

$$M\left(\underset{\sim}{\theta},t\right) = \sum_{j=1}^{m} G_g\Big(a_j,c_j,d_j,e_j,f_j,t\Big) \tag{3.1}$$

Where each Gauss function is expressed by:

$$G_g(a,c,d,e,f,t) = f \,.\, e^{\left(\frac{\pi^2(t-a)^2}{d^2(\pi+2atan(-e(t-a)))^2}\right)^c} \tag{3.2}$$

Where a is the time location or relative position of the Gauss function, c is the kurtosis which is a measure of the ”peakedness” of the function, d is width or aperture, e is the skew or inclination, f is the amplitude of the Gauss function and t is time.

The template is a first rough description of the measured signal, which is defined by an initial set of parameters for each Gauss function. It is this first approximation that will be adapted to fit the signal as perfectly as possible, by the use of the iterative method.

The mathematical problem at hand consists in finding the set of model parameters that more closely approximate the observed time series. This problem can be interpreted as a least squares fitting problem. Generally the least squares method works by adjusting the parameters of a model function in order to minimize the error or distance, between the model and the measured signal that is to be represented by it.
Considering a set of n measured data points $(t_i,y_i), i = 1,\ldots,n$, where t_i is the independent variable, which in this case is time, and y_i is the dependent variable, that is measured through time, in this case we measure the electrical potential in the surface of the heart. The model function has the form $M(\underset{\sim}{\theta},t)$ as expressed in 3.1, where $\underset{\sim}{\theta}$ is a vector that groups the $m\times$five adjustable parameters.
The objective is to find the set of model parameters that best fit the measured data, and by the least squares method the best set is the one that minimizes the sum S of squared

residuals:

$$S = \sum_{i=1}^{n} r_i^2 \tag{3.3}$$

The residual or error is defined as the difference or distance between the measured values of the dependent variable y_i and the estimated values predicted by the model $M(\underset{\sim}{\theta},t)$, it can be expressed as:

$$r_i = y_i - M(\underset{\sim}{\theta},t) \tag{3.4}$$

The same equation can be expressed in the matrix form as follow:

$$\underset{\sim}{\varepsilon} = \underset{\sim}{z} - \underset{\sim}{z}_R \tag{3.5}$$

where $\underset{\sim}{\varepsilon}$ is an array that groups the residual for each time point, as stated bellow:

$$\underset{\sim}{\varepsilon} = \left[\varepsilon_1,\ldots,\varepsilon_n\right]^T \tag{3.6}$$

and in turn, $\underset{\sim}{z}_R$ represents the model as stated in 3.1:

$$\underset{\sim}{z}_R = M(\underset{\sim}{\theta},\underset{\sim}{t}) \tag{3.7}$$

$\underset{\sim}{\theta}$ is the array that groups the model parameters that we want to calculate and that are to be iteratively adapted by successive approximation to better fit the measured signal.

$$\underset{\sim}{\theta} = \left[a,c,d,e,f\right]^T \tag{3.8}$$

The cost function $\chi(\underset{\sim}{\varepsilon})$ in matrix form is equivalent to S in 3.3.

$$\chi(\underset{\sim}{\varepsilon}) = \underset{\sim}{\varepsilon}^T\underset{\sim}{\varepsilon} \tag{3.9}$$

It is the equation in 3.9 that is to be minimized and that minimum is found by setting the gradient to zero.

$$\frac{\partial \chi(\underset{\sim}{\varepsilon})}{\partial \underset{\sim}{\theta}} = 0 \tag{3.10}$$

If we substitute in the cost function 3.9 the error as stated in 3.5, and in turn express it in terms of the model in 3.7 we obtain the cost function dependency on the model parameters:

$$\chi = \left(\underset{\sim}{z} - M(\underset{\sim}{\theta},\underset{\sim}{t})\right)^T \left(\underset{\sim}{z} - M(\underset{\sim}{\theta},\underset{\sim}{t})\right) \tag{3.11}$$

$$\chi = \left(\underset{\sim}{z}^T\underset{\sim}{z} - 2\,\underset{\sim}{z}^T M(\underset{\sim}{\theta},\underset{\sim}{t}) + M(\underset{\sim}{\theta},\underset{\sim}{t})^T M(\underset{\sim}{\theta},\underset{\sim}{t})\right) \tag{3.12}$$

In order to determine the parameters that minimize the cost function and going back to equation 3.10 [1]:

$$\begin{aligned}
\frac{\partial \chi(\underset{\sim}{\varepsilon})}{\partial \underset{\sim}{\theta}} &= \frac{\partial\left(\underset{\sim}{z}^T\underset{\sim}{z}\right)}{\partial \underset{\sim}{\theta}} - \frac{\partial\left(2\,\underset{\sim}{z}^T\underset{\sim}{M}\right)}{\partial \underset{\sim}{\theta}} + \frac{\partial\left(\underset{\sim}{M}^T\underset{\sim}{M}\right)}{\partial \underset{\sim}{\theta}} \\
&= -2\,\underset{\sim}{z}^T\frac{\partial \underset{\sim}{M}}{\partial \underset{\sim}{\theta}} + \frac{\partial \underset{\sim}{M}^T}{\partial \underset{\sim}{\theta}}\underset{\sim}{M} + \underset{\sim}{M}^T\frac{\partial \underset{\sim}{M}}{\partial \underset{\sim}{\theta}} \\
&= -2\,\underset{\sim}{z}^T\frac{\partial \underset{\sim}{M}}{\partial \underset{\sim}{\theta}} + 2\frac{\partial \underset{\sim}{M}^T}{\partial \underset{\sim}{\theta}}\underset{\sim}{M}
\end{aligned} \tag{3.13}$$

$$\frac{\left(\partial \underset{\sim}{M}\right)^T}{\partial \underset{\sim}{\theta}}\underset{\sim}{M} = \underset{\sim}{z}^T\frac{\partial \underset{\sim}{M}}{\partial \underset{\sim}{\theta}} \tag{3.14}$$

$$\underset{\sim}{J}_M = \underset{\sim}{z}^T\frac{\partial \underset{\sim}{M}}{\partial \underset{\sim}{\theta}} \tag{3.15}$$

$$\underset{\sim}{J}_M^T \,.\, \underset{\sim}{M} = \underset{\sim}{z}^T \,.\, \underset{\sim}{J}_M \tag{3.16}$$

[1] $M(\underset{\sim}{\theta},\underset{\sim}{t}) = \underset{\sim}{M}$

The normal equations in 3.16 are non-linear on the parameters $\underset{\sim}{\theta}$ therefore they don't have an analytical closed solution. For this reason, iterative methods will be used to find an estimation for the parameters that minimize the cost function in equation 3.9.
The iterative method to be used is called the Levenberg-Marquardt compromise which as the name suggests is a compromise between two different methods, the Gradient or Steepest Descent and the Gauss-Newton methods.
Most iterative algorithms involve choosing a set of initial values for the parameters, which are progressively refined by successive approximation, preferably converging to a global minimum of the cost function. The iterative process can be expressed by:

$$\underset{\sim}{\hat{\theta}}^{i} = \underset{\sim}{\hat{\theta}}^{(i-1)} + \nu(\underset{\sim}{\theta}^{(i-1)}) \tag{3.17}$$

Where $\underset{\sim}{\hat{\theta}}^{i}$ is the iteration i, which results from the previous iteration plus the director function $\nu(\underset{\sim}{\theta}^{(i-1)})$. The director function ν establishes the progression direction of successive estimation vectors in the parameter multidimensional space.

3.3.1 Gradient Method

The Gradient or Steepest descent method is a simple way to iteratively find a local minimum of a function using gradient descent. In this method the walk through the parameter space in the direction of the solution is made using steps proportional to the negative of the cost function's gradient at each point, the procedure is known as gradient descent. By following the opposite of the gradient vector (which is the direction of greatest positive variation), it is guaranteed to end up in a local minimum of the cost function, if it exists.
In this case, the director function ν is proportional, with proportionality constant η, to the opposite of the cost function's gradient in each iteration, *i.e.*,

$$\underset{\sim}{\nu} = -\eta \nabla \chi(\underset{\sim}{\varepsilon}), \tag{3.18}$$

Where ∇ is the gradient as stated below:

$$\nabla = \left[\frac{\partial}{\partial\theta_1}, \cdots, \frac{\partial}{\partial\theta_n}\right], \quad n = 5 \tag{3.19}$$

The equation for the iterative process in 3.17 can now be adapted for the Gradient method

using the director function in 3.18,

$$\underset{\sim}{\hat{\theta}}^{i} = \underset{\sim}{\hat{\theta}}^{(i-1)} - 2\,\eta\,\underset{\sim}{J}_{M}^{T(i-1)}\left(\underset{\sim}{M}^{(i-1)} - \underset{\sim}{z}\right) \tag{3.20}$$

Where $\underset{\sim}{J}_{M}^{T(i-1)}$ is the Jacobian Matrix of M calculated for $\underset{\sim}{\hat{\theta}}^{(i-1)}$.
The proportionality constant η combined with the cost's scalar field slope, quantified by the Jacobian matrix, determines the width of each iteration or the convergence velocity of the method 3.21. This parameter η can be stationary or it can be adapted along the iterative process, and either way it greatly affects the convergence behavior of the method.
If is small enough the steps of the iterative process are also small and $\underset{\sim}{\hat{\theta}}$ follows a overdamped, smooth path in the parameters space, towards the solution. Otherwise, if η is bigger, the steps of the iterative process are also bigger and the route towards the solution is irregular or underdamped. In the limit, if η is too big, the algorithm becomes unstable and diverges.

$$\left|\underset{\sim}{\hat{\theta}}^{i} - \underset{\sim}{\hat{\theta}}^{(i-1)}\right| = \eta \cdot \left|\nabla\,\chi\left(\underset{\sim}{\varepsilon}^{(i-1)}\right)\right| \tag{3.21}$$

The gradient method is robust but sometimes slow. It can find a minimum of the cost function (but not necessarily the global minimum), even starting from a relatively poor initial condition, the downside is that it can take a while to get there.

3.3.2 Gauss-Newton Method

$$\underset{\sim}{z} = \underset{\sim}{z}_{R} + \underset{\sim}{\varepsilon}, \tag{3.22}$$

The Gauss-Newton method is also called linearization method because the model function used to describe the measured signal, in this case $\underset{\sim}{z}_{R} = M(\underset{\sim}{\theta},t)$, is approximated by a Taylor series expansion, limited to the first term and centered in the current estimate of the parameters vector, as stated bellow:

$$M(\underset{\sim}{\hat{\theta}} + \underset{\sim}{\delta}_{\theta}) \simeq M(\underset{\sim}{\hat{\theta}}) + \nabla M \,.\, \underset{\sim}{\delta}_{\theta} \tag{3.23}$$

The parameter $\underset{\sim}{\delta}_{\theta}$ represents the increment that is added to the model parameters vector.

Because the relation between the model $\underset{\sim}{M}$ and the error $\underset{\sim}{\varepsilon}$ established in 3.22, the linearization of the model stated in 3.23 implies also a linearization of the error function centered in the current estimate of the parameters vector,

$$\varepsilon(\underset{\sim}{\hat{\theta}} + \underset{\sim}{\delta}_{\theta}) \simeq \varepsilon(\underset{\sim}{\hat{\theta}}) + \nabla \underset{\sim}{\varepsilon} \,.\, \underset{\sim}{\delta}_{\theta} = \varepsilon(\underset{\sim}{\hat{\theta}}) - \nabla M \,.\, \underset{\sim}{\delta}_{\theta} \tag{3.24}$$

The direction of the incremented parameter vector $(\underset{\sim}{\hat{\theta}} + \underset{\sim}{\delta}_{\theta})$ needs to comply with the cost function minimization criteria as established in 3.10.

$$\frac{\partial \chi(\underset{\sim}{\hat{\theta}}^{(i)})}{\partial \underset{\sim}{\delta}_{\theta}} = \frac{\partial \chi(\underset{\sim}{\hat{\theta}}^{(i+1)} + \underset{\sim}{\delta}_{\theta})}{\partial \underset{\sim}{\delta}_{\theta}} = 0, \tag{3.25}$$

Where $\underset{\sim}{\delta}_{\theta}$ is the director function of the iterative process:

$$\underset{\sim}{\nu} = \underset{\sim}{\delta}_{\theta} \Rightarrow \underset{\sim}{\hat{\theta}}^{(i)} = \underset{\sim}{\hat{\theta}}^{(i-1)} + \underset{\sim}{\delta}_{\theta} \tag{3.26}$$

Evoking again the least squares criteria that needs to be complied by the cost function:

$$\chi(\underset{\sim}{\varepsilon}) = \underset{\sim}{\varepsilon}^{T} \,.\, \underset{\sim}{\varepsilon} \tag{3.27}$$

From equation 3.25 it is possible to derive the increment $\underset{\sim}{\delta}_{\theta}$ that minimizes the cost function.

$$\underset{\sim}{\delta}_{\theta} = \left(\underset{\sim}{J}_{M}^{T(i-1)} \,.\, \underset{\sim}{J}_{M}^{(i-1)}\right)^{-1} \,.\, \underset{\sim}{J}_{M}^{T(i-1)} \left(\underset{\sim}{z} - \underset{\sim}{M}^{(i-1)}\right) \tag{3.28}$$

Inserting $\underset{\sim}{\delta}_{\theta}$ as calculated in 3.28 in equation 3.26 results in a new estimate for the parameters vector and another step in the iterative process, preferably in the direction of the minimum of the parameters space. This minimum is only guaranteed to be the global one if it is unique, otherwise the Gauss Newton method can converge to any local minimum. The method is also quite sensitive to the quality of the set of initial conditions, this happens due to the relatively narrow band in which the linearization of the model can be considered as good approximation. Despite this the method is quite fast, especially once it gets close to the solution.

3.3.3 Levenberg-Marquardt Compromise

Combining the properties of the Gradient method, that is robust in terms of the initial conditions but slow in the final approach to the solution, with the properties of the Gauss-Newton method that is sensitive to the initial conditions but fast once it gets close to the solution, it is possible to create a new method that combines the advantages of both without the limitations of either one. This new method was first explored by Kenneth Levenberg and published in 1944, and latter revisited by Donald Marquardt who published his work in 1963.
The method is currently known as the Levenberg-Marquardt compromise and it interpolates between the Gauss-Newton algorithm and the method of gradient descent.

The director function for this method derives from geometrical interpretation of the director functions of the Gradient and Gauss-Newton methods, and it combines both functions:

$$\underset{\sim}{\nu}_{M} \equiv \underset{\sim}{\delta}_{\theta} = \left(\underset{\sim}{J}_{M}^{T^{(i-1)}} . \underset{\sim}{J}_{M}^{(i-1)} + \zeta \underset{\sim}{I}\right)^{-1} . \underset{\sim}{J}_{M}^{T^{(i-1)}} \left(\underset{\sim}{z} - \underset{\sim}{M}^{(i-1)}\right) \tag{3.29}$$

The parameter ζ is a positive constant called damping coefficient. When ζ is small or zero the director function in 3.29 becomes identical to the director function for the Gauss-Newton method 3.26, and when the damping coefficient is bigger, the same function becomes identical to the director function for the Gradient method 3.18.

The damping coefficient ζ normally starts with a bigger value, close to one, in order to take advantage of the robust behavior of the Gradient method when far from the solution. And it is progressively reduced, once the paremeters estimation gets closer to the solution and the linear approximation given by the Gauss-Newton method improves. This way the final convergence takes advantage of the increased convergence velocity of the Gauss-Newton method when it gets close to the solution.
In order to quantify the quality of the linear model derived by the Gauss-Newton method the linearity coefficient ρ_ι is defined as:

$$\rho_\iota = \frac{\chi\left(\underset{\sim}{\hat{\theta}}^{(i-1)}\right) - \chi\left(\underset{\sim}{\hat{\theta}}^{(i-1)} + \underset{\sim}{\delta}_{\theta}\right)}{\chi\left(\underset{\sim}{\hat{\theta}}^{(i-1)}\right) - \chi_\iota\left(\underset{\sim}{\hat{\theta}}^{(i-1)} + \underset{\sim}{\delta}_{\theta}\right)}, \tag{3.30}$$

Where χ is the cost function as stated in equation 3.9,

$$\chi\left(\hat{\underset{\sim}{\theta}}^{(i-1)}\right) = \underset{\sim}{\varepsilon}^T . \underset{\sim}{\varepsilon} = \left(\underset{\sim}{z} - \underset{\sim}{M}^{(i-1)}\right)^T \left(\underset{\sim}{z} - \underset{\sim}{M}^{(i-1)}\right) \tag{3.31}$$

and χ_ι is the cost function for the linearized model:

$$\chi_\iota\left(\hat{\underset{\sim}{\theta}}^{(i-1)} + \underset{\sim}{\delta}_\theta\right) = \underset{\sim}{\varepsilon}_\iota^T . \underset{\sim}{\varepsilon}_\iota = \left(\underset{\sim}{z} - \underset{\sim}{M}^{(i-1)} - \underset{\sim}{J}_M^{T^{(i-1)}} . \underset{\sim}{\delta}_\theta\right)^T \left(\underset{\sim}{z} - \underset{\sim}{M}^{(i-1)} - \underset{\sim}{J}_M^{T^{(i-1)}} . \underset{\sim}{\delta}_\theta\right) \tag{3.32}$$

The expression for the linearity coefficient in 3.30, can be simplified to:

$$\rho_\iota = \frac{\chi\left(\hat{\underset{\sim}{\theta}}^{(i-1)}\right) - \chi\left(\hat{\underset{\sim}{\theta}}^{(i-1)} + \underset{\sim}{\delta}_\theta\right)}{\underset{\sim}{\delta}_\theta^T \left[\underset{\sim}{J}_M^{T^{(i-1)}} . \left(\underset{\sim}{z} - M^{(i-1)}\right) + \zeta \underset{\sim}{\delta}_\theta\right]}, \tag{3.33}$$

The denominator in equation 3.33 is always positive, so for $\rho_\iota > 0$:

$$\rho_\iota > 0 \Rightarrow \chi\left(\hat{\underset{\sim}{\theta}}^{(i-1)}\right) > \chi\left(\hat{\underset{\sim}{\theta}}^{(i-1)} + \underset{\sim}{\delta}_\theta\right) \Leftrightarrow \chi^{(i)} < \chi^{(i-1)}. \tag{3.34}$$

Which mean that for $\rho\iota > 0$ the iterative process evolves in the direction of the minimization of the cost function. This desired behavior can be sated as a condition for the next iteration:

$$\hat{\underset{\sim}{\theta}}^{(i)} = \hat{\underset{\sim}{\theta}}^{(i-1)} + \underset{\sim}{\delta}_\theta \Leftarrow \rho_\iota > 0. \tag{3.35}$$

Based on the arguments stated above the evaluation procedure of the damping coefficient as an alternating factor between the Gradient and Gauss-Newton methods can be formulated as proposed by Marquardt,

The constant ρ_∇ quantifies the stage bellow which the method closely resembles the Gradient method and correspondingly, ρ_G quantifies the stage above which the method more closely resembles the Gauss-Newton method. The constants κ_1 and κ_2 translate the ascending and descending alternation rhythms. These constants were set by Marquardt to: $\rho_\nabla = 0.25$; $\rho_G = 0.75$; $\kappa_1 = 2$ and $\kappa_2 = 3$.

More recently a new criterion for the evaluation of the damping coefficient was presented, that in most cases shows to be faster then the former, and for that reason is the one to be used in this particular problem:

$$
\begin{array}{rcl}
\text{calculate} & : & \underset{\sim}{M}^{(i)},\ \underset{M}{\underset{\sim}{J}}^{(i)},\ \rho_\iota \\
 & & \\
\rho_\iota < \rho_\nabla & : & \zeta = \kappa_1 \,.\, \zeta \\
\rho_\iota > \rho_G & : & \zeta = \zeta / \kappa 2 \\
\rho_\iota > 0 & : & \underset{\sim}{\hat{\theta}}^{(i+1)} = \underset{\sim}{\hat{\theta}}^{(i)} + \underset{\theta}{\underset{\sim}{\delta}}
\end{array}
$$

Table 3.2: Damping coefficient adaptation algorithm as proposed by Marquardt

$$
\begin{array}{rcl}
\text{calculate} & : & \underset{\sim}{M}^{(i)},\ \underset{M}{\underset{\sim}{J}}^{(i)},\ \rho_\iota \\
 & & \\
\rho_\iota > 0 & : & \underset{\sim}{\hat{\theta}}^{(i+1)} = \underset{\sim}{\hat{\theta}}^{(i)} + \underset{\theta}{\underset{\sim}{\delta}} \\
 & : & \zeta = \zeta \,.\, \max\left(1/\kappa 2,\ 1 - \left(\kappa 1 - 1\right)\left(2\,\rho_\iota - 1\right)^{\kappa 3}\right) \\
 & : & \kappa = \kappa 1 \\
\rho_\iota \leq 0 & : & \zeta = \zeta \,.\, \kappa 4 \\
 & : & \kappa 4 = 2 \,.\, \kappa 4
\end{array}
$$

Table 3.3: Damping coefficient adaptation algorithm as proposed by Nielsen

In this algorithm the constants $\kappa_1 \ldots \kappa_4$ are initialized as: $\kappa_1 = 2$; $\kappa_2 = 3$; $\kappa_3 = 3$ and $\kappa_4 = 2$.

3.3.4 Computational Algorithm

The computational algorithm used for data analysis is directly derived from the Levenberg-Marquardt compromise described above. It is an adaptation of the algorithm previously published [43], further developed for the current application.

First the MAP measured signal is segmented into individual atrial activations. This is accomplished by means of a correlation with a simplified template designed for high correlation specifically with the main deflection of the MAP. This segmentation allows calculating the period of each atrial activation and thus its instantaneous frequency.
A specific template designed to identify the features of the MAP signals is scaled to the period and amplitude of each signal segment. This scaled template is the initial condition

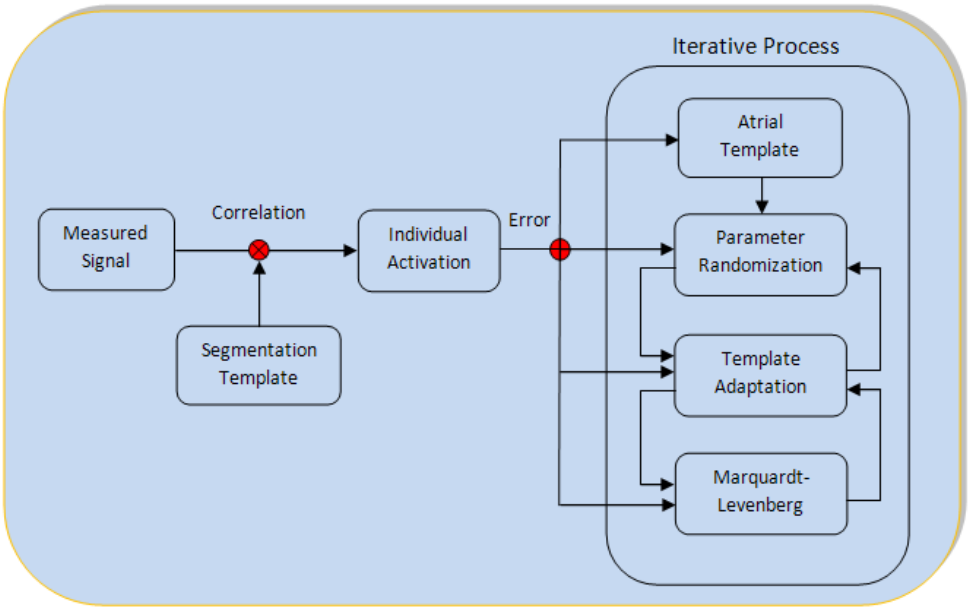

Figure 3.1: Computational algorithm scheme

of the parameter identification process. The process of finding the set of Gauss function parameters that best fit the measured signal starts with a randomized grid search. If this randomized search is able to create a closer fit to the measured signal then the initial template, the template is updated with the randomized parameters. The result of the grid search is then feed to the iterative Levenberg-Marquardt process described in the previous section. For each iteration the Jacobean matrix and the linearity coefficient are calculated in order to determine the direction of the director function. In all the steps the fitting error between the current version of the Gaussian model and the measured signal is quantified in order to evaluate the convergence of the process.

The algorithm returns the number of analysed atrial activations, the average frequency and standard deviation of atrial activations, the set of Gauss function coefficients that best describe each atrial activation, the error of each fit and the time interval of each segment.

Chapter 4

Results

In this chapter the results from the gene expression analysis and the electrophysiological signal measurements and analysis will be presented.

4.1 Gene Expression Analysis

Gene expression analysis was performed in groups, designated pools, comprising the samples referent to five animals subjected to the same experimental conditions. For each experimental condition - three different periods of pacing and three different periods of control - two five animal pools were analysed. The gene expression analysis by mRNA quantification was performed in both the right and left atria. Although only the right atria were subjected to rapid pacing, its effects were also investigated in the left atria.
This approach allows for normalization of the results from pacing experiments, not only against the control genes, as described in the previous chapter, but also against the experimental control groups that underwent similar surgery periods. The experimental approach is therefore cancelled, by this normalization procedure, as a possible contributing factor for the gene expression variations.

The following graphics present the averaged results of the two pools, normalized for both the expression of a control gene, mentioned in the previous chapter and the expression levels of experimental control groups.

The graphic in figure 4.1 and figure 4.2 show the relative expression of all ten analysed genes, for the right and left atria respectively. In both these graphics the vertical axis represents relative expression, where 1 stands for unchanged expression level. Despite

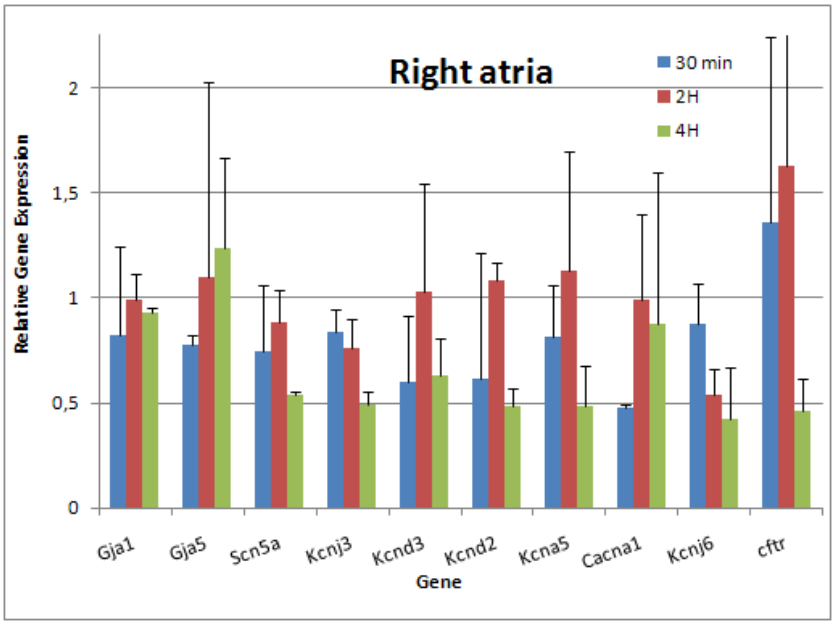

Figure 4.1: Right Atria Gene Expression Results

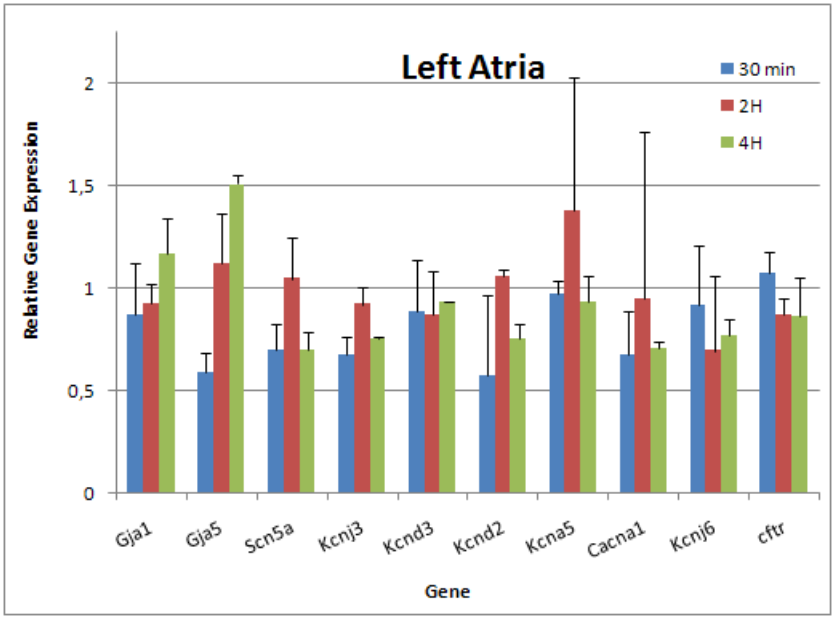

Figure 4.2: Left Atria Gene Expression Results

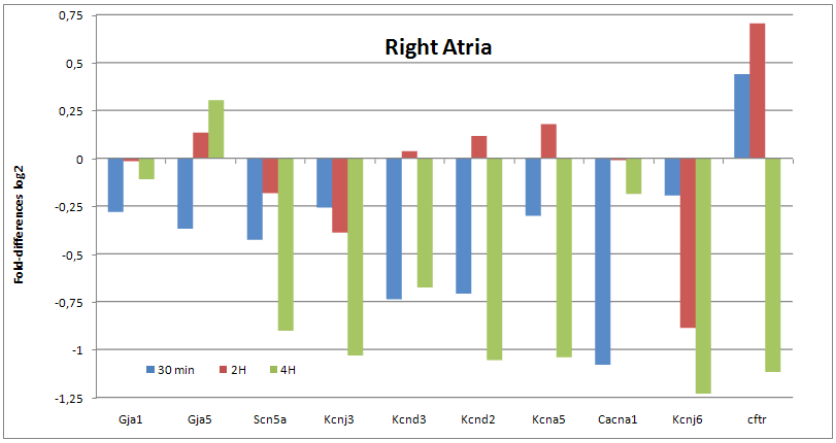

Figure 4.3: Right Atria Gene Expression Results

the considerable error margins, especially in the results referent to the right atria, it is possible to notice greater expression changes in the right atria, when compared to the left atria. It is also evident that the error associated with the quantification of mRNA is considerably lower in the samples referent to the four hours of pacing groups.

The graphics in figures 4.3 and 4.4 show the same results in a logarithmic scale, where zero stands for unchanged expression, negative values stand for underexpression and positive values overexpression of the analysed genes. Once again it is clear that the right atrium was quite more affected by the rapid pacing when compared with the left, most of the changes being the underexpression of genes when compared to the control conditions. Even in the right atria, there seems to be some genes that are almost unaffected by the rapid pacing, like the ones that code for connexions, Gja1 and Gja5. On the contrary, some genes have quite significant changes in expression levels like Cacna1, Kcnj6 or cftr. Analyzing the results of the right atria in a time evolution perspective, it is possible to identify genes like Kcnj3 and Kcnj6 which had a clear evolution of underexpression throughout the different periods of pacing, showing a quite significant drop in expression levels, to less then half, at the end of four hours of pacing. Other genes expression levels have a less linear evolution, like Kcnd2, Kcnd3 and Cacna1, which start by being underexpressed at thirty minutes of pacing, close to unchanged expression after two hours and again underexpression at the end of four hours.
None of the gene expression levels reported surpasses a $\pm$ 75% change regarding the control condition.

The gene Gja1 coding for the connexin-43 was slightly underexpressed in all three periods of pacing, showing an unclear progression in the right atria, and in the left atria it was

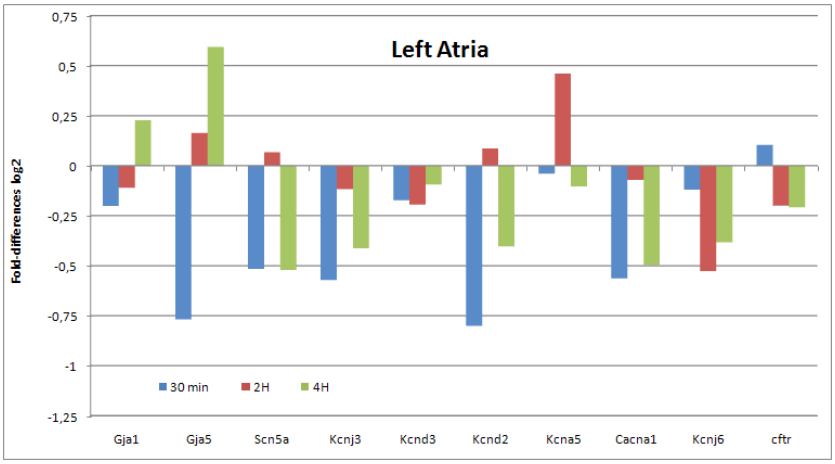

Figure 4.4: Left Atria Gene Expression Results

underexpressed at 30 minutes and 2 hours of pacing but overexpressed after 4 hours of pacing. The expression changes for this gene were minor, never higher than 30%.
Connexin-40 coded by the Gja5 gene presented more significant changes in expression levels. It starts being underexpressed at 30 minutes of pacing progressing for crescent overexpression at 2 and 4 hours of pacing. The behavior is the same in both right and left atria, but more pronounced in the left atria, reaching differences of up to 50% in expression levels.

The genetic expression results for gene Scn5a coding for a sodium channel all point in the direction of underexpression, reaching levels of 50% the control expression in the right atria after 4 hours of pacing. However the progression is not linear since it starts with marked underexpression at 30 minutes of pacing, returning at 2 hours to control levels and finally confirming the underexpression tendency after 4 hours of pacing. These results are quite significant, showing a low statistical dispersion between the samples.

The results found for the Kcnd2 and Kcnd3 genes coding for the Kv4 potassium channel are similar in nature, presenting a underexpression at 30 minutes, a very slight overexpression that can be interpreted as unchanged expression levels at 2 hours of pacing and finally a pronounced underexpression after 4 hours of pacing, reaching a minimum of -52% mRNA concentration. For both genes in both atria, the statistical dispersion between the two pools decreased significantly with increasing pacing periods.

The Kv1.5 channel coded by the Kcna5 gene is the major contributor for the I_{Kur} current. It was found to be underexpressed in the right atria at 30 minutes of pacing, slightly overexpressed at 2 hours and considerably underexpressed after 4 hours of pacing. In the left atria the behaviour is quite different, since the expression is unchanged at 30 minutes

	Right atria			Left Atria		
Genes	**30 minutes**	**2 hours**	**4 hours**	**30 minutes**	**2 hours**	**4 hours**
Gja1	-0.281	-0.016	-0.110	-0.202	-0.111	0.228
Gja5	-0.369	-0.134	0.304	-0.769	0.164	0.594
Scn5a	-0.427	-0.183	-0.902	-0.516	0.066	-0.521
Kcnd2	-0.708	0.117	-1.056	-0.801	0.085	-0.403
Kcnd3	-0.738	0.037	-0.676	-0.173	-0.195	-0.094
Kcna5	-0.302	0.178	-1.041	-0.040	0.461	-0.104
Cacna1	-1.081	-0.010	-0.187	-0.564	-0.071	-0.496
Kcnj3	-0.258	-0.389	-1.032	-0.572	-0.118	-0.413
Kcnj6	-0.195	-0.888	-1.232	-0.121	-0.527	-0.383
Cftr	0.439	0.705	-1.118	0.104	-0.200	-0.208

Table 4.1: Right and left atria gene expression results in $\log_2$ scale

and 4 hours and overexpressed at 2 hours of pacing. Most of the results for this gene present a very large statistical dispersion between the samples.

The calcium L-type channel coded by the Cacna1 gene is one of the most important ion channels in the modulation of cardiac action potential duration and consequently, cardiac ERP. This gene was found to be underexpressed or unchanged over all periods of pacing and both atria. At 30 minutes of pacing it presents maximum underexpression for both atria, reaching -50% in the right atria. After 2 hours of pacing the expression returns to control levels and at 4 hours of pacing it returns to underexpression although not so pronounced as at the first period. The expression results for this gene have considerable statistical dispersion especially for the 2 hours of pacing groups.

The genes Kcnj3 and Kcnj6 coding for the acetylcholine dependent Kir3 family channels are underexpressed in both atria and all time periods. The results are clearer in the right atria, where there is a clear progression of crescent underexpression beginning at 30 minutes of pacing with about -25% and reaching -50% and -60% of underexpression for the two genes after 4 hours of pacing. These results show moderate statistical dispersion between the samples.

Finally, the Cftr gene coding for a Cl^- channels was found to be almost unchanged in the left atria, while in the right one it shows first a considerable increase in expression at 30 minutes and 2 hours of pacing and the a clear underexpression after 4 hours of pacing, reaching about -50%. The results for the right atria present enormous statistical dispersion.

4.2 Signal Measurements

Atrial activation signals were measured using the unipolar monophasic action potential method as specified in chapter 2. The measurement setup was developed during the course of the experiments, evolving from initial electrogram-like biphasic signals to the action potential-like monophasic signals in the final experiments. The quality of the measured signal depends greatly on the position and pressure exerted by the recording electrode placed on the atrial surface. For this reason, different signals measured in different experiments can have different morphology. Some of the measures did not meet the requirements for the parametric signal analysis, and thus were not used.

One of the disturbing factors that can influence the morphology of the measured atrial activation is the interfering ventricular activation, which occurs in the end of the repolarization phase of the atrial action potential. This interference can be minimized by placing the recording electrode as far as possible of the ventricle, which is not always possible due to the natural variations in heart position and exposure during the experimental procedure.

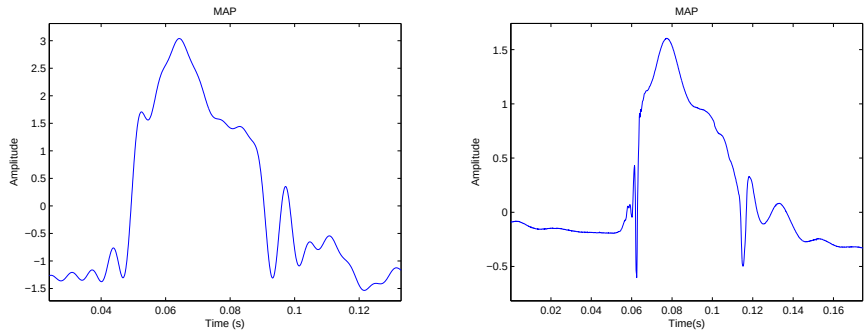

(a) (b)

Figure 4.5: Examples of measured MAP signals

As it can be observed in the examples in figure 4.5, the morphology of the measured signals can be quite diverse. Several aspects of the atrial activation signal vary between measures, namely the baseline oscillations, the influence of the ventricular signal and the artefacts during phase 1 upslope.

The feature that is maintained throughout most of the recordings, which is the most important for the evaluation of MAP, is the main accident's shape. The wide positive deflection contains most of the useful information about duration, phase 1 upslope and phase 4 down slope of the underlying action potential.

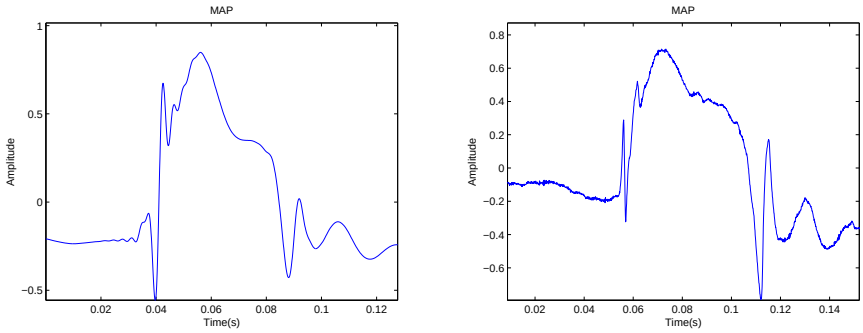

(a) (b)

Figure 4.6: Examples of measured MAP signals

Recordings in which this deflection was not reasonably conserved were not considered for the parametric signal analysis.

4.3 Data Analysis

In this section the results of the iterative fitting algorithm are presented together with the model parameter changes evaluated before and after the rapid atrial pacing.

The algorithm was applied to 50 segments of atrial MAP signal corresponding to small time periods before and after rapid atrial pacing. This procedure allows for a comparison between the model parameters found before and after atrial pacing and consequently, a characterization of the atrial ionic remodelling that could have happen in between. Several templates, with a different number of Gauss functions, were developed in accordance with the variation in morphology of the measured signals (figure 4.7), in order to compose the best possible first approximation to the signal.

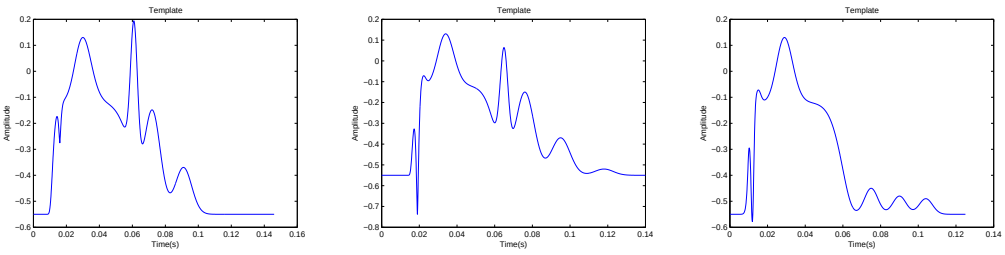

(a) (b) (c)

Figure 4.7: Templates

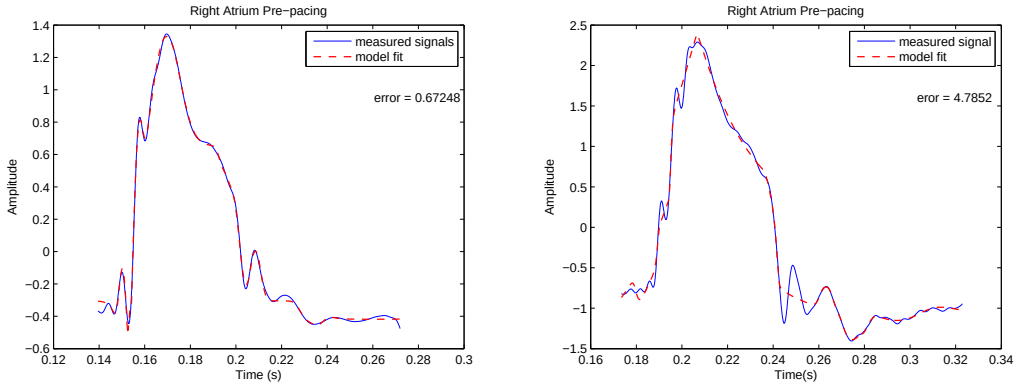

(a) (b)

Figure 4.8: Fitted Model

The iterative fitting process converged to a solution in all the tested signals and the quality of this solution can be evaluated by the quadratic error of the final approximation. The error averaged 1.9167, SD = 2.4934. The error varied with the quality of the measured signal and the number of parameters considered in the initial template. Examples shown in figure 4.8 clearly demonstrate the very close approximation accomplished with this fitting algorithm, even in the case of figure 4.8 b), where the fitting error was considerably above average.

The results represented in figures 4.9 and 4.10 show the evolution of the analysed parameters for the Gauss function that models the main positive deflection of the atrial MAP. Where CC parameter stands for kurtosis, which is a measure of “peakedness”, DD stands for the width of the function, EE stands for skew or inclination and FF stands for amplitude. This analysis was performed for three different pacing periods, 30 minutes, 2 hours and 4 hours. The results were normalized against the same parameters obtained for the control experiments in order to discard the possible influence of experimental condition and isolate the influence of rapid atrial pacing.

It is possible to notice in the graphic on figure 4.10 that most of the parameters analysed do not have a clear progression throughout the three pacing periods.

Kurtosis represented by the parameter CC is significantly increased after 30 minutes of rapid pacing. At 2 hours of pacing it is considerably decreased and after 4 hours it returns to near control levels. A decreased kurtosis corresponds to a more pointy triangular shaped potential with slower slopes.

The width of the modelling Gauss function, represented by the DD parameter is decreased in the two first periods of pacing and slightly increased at 4 hours of pacing. Additionally

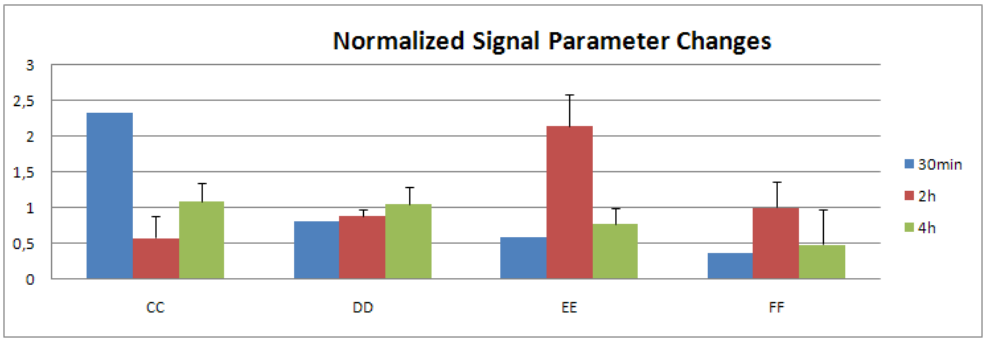

Figure 4.9: Right Atria Parameter Changes

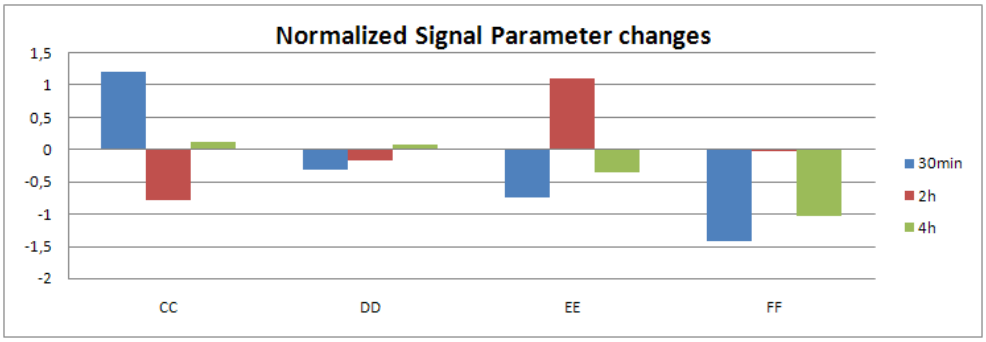

Figure 4.10: Right Atria Parameter Changes in log scale

an increasing tendency can be noticed. The width of the modelling function is closely related to the duration of the cardiac action potential being modelled. Although the increase at 4 hours might seem small, even a small variation in this parameter can be easily noticeable in the modelled signal as is shown in figure 4.11.

The skew of the function represented by EE is decreased after 30 minutes of rapid pacing and increased after 2 hours. At 4 hours this parameter is slightly decreased again. The

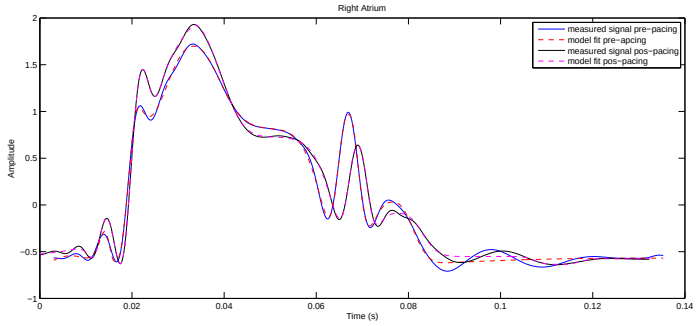

Figure 4.11: Right Atrium signal and fit model before and after 4 hours of pacing

Right atria			
Parameters	**30 minutes**	**2 hours**	**4 hours**
CC	1.220	-0.784	0.118
DD	-0.310	-0.172	0.077
EE	-0.746	1.100	-0.361
FF	-1.422	0.007	-1.028
HR	0.102	0.073	0.304

Table 4.2: Right atria parameter variation results in $\log_2$ scale. HR: heart rate

skew of the curve measures the tilt or inclination of the Gauss function. This parameter was negative for all segments analysed which indicates a left tilt of the function. It can be related with the slope of the repolarization phase of the action potential. Decreased skew means less left tilt, which in term means a faster repolarization phase.

The amplitude of the Gauss function is considerably decreased in relation to control experiments at 30 minutes and 4 hours of pacing. After 2 hours it remains unchanged. The amplitude of the signal is correlated with the amplitude of the action potential.

Chapter 5

Discussion

5.1 Gene Expression Analysis

The results of the gene expression analysis add significant information concerning the early stages of atrial ionic remodelling and show that even in such short periods of time the genetic regulation machinery can, in some cases, start to have measurable effects in the expression of cardiac ion channels.

The results of the gene expression analysis are in most cases in agreement with similar data published in recent literature. Since most studies of gene expression quantification in the context of AF are performed in animal models of chronic rapid atrial pacing (>1 day) or patients with long term persistent AF, the comparison can only be made by interpolation of the results found for the three short pacing periods evaluated.

Current	Channel	Genes	Results at 4 hours	Literature Results
all	connexin-40,43	Gja5, Gja1	underexpression,overexpression	underexpression/lateralization
I_{Na}	Nav1.5	Scn5a	underexpression	underexpression
I_{to}	Kv4.2, Kv4.3	Kcnd2, Kcnd3	underexpression	underexpression
I_{Kur}	Kv1.5	Kcna5	underexpression	underexpression/overexpression
I_{CaL}	L-type Ca^{2+}	Cacna1	underexpression	underexpression
I_{KAch}	Kir3.1, Kir3.2	Kcnj3, Kcnj6	underexpression	underexpression/unchanged
I_{Cl}	Cftr	Cftr	overexpression/underexpression	

Table 5.1: Comparison between results obtained for the right atria after 4 hours of pacing *vs* published data

Results for the genes Gja5 and Gja1 coding for connexins Cx40 and Cx43 respectively were not in total agreement with published data. Connexins Cx40 and Cx43 are the most abundant connexins in the heart tissue and its influence in atrial remodelling was already

investigated in the context of AF in a goat model of chronic atrial pacing [21]. This study by van der Velden reported a reduced amount of protein (up to 50%) for both species accompanied by heterogeneous distribution of Cx40. Surprisingly, the protein underexpression was not validated by decreased mRNA levels, these remained unchanged. This author measured not only the mRNA levels of the genes coding for these connexins but also the protein levels and its distribution along the atrial miocytes, which were found to be heterogeneous after atrial pacing. In fact the distribution of connexins is also a factor that affects the conduction of the action potentials.
This study is atypical in the sense that the protein levels were not backed up by according mRNA levels. This fact demonstrates the hypothesis of ulterior mechanisms to mRNA transcription, modulating the actual expression of functional protein.

The expression changes presented in the previous chapter for Cx43 are quite small and due to the considerable statistical dispersion cannot be interpreted as significant. The maintenance of mRNA levels for Cx43 points to the hypothesis of sole post-transcriptional downregulation of this protein, from short to long periods of pacing.
Connexin Cx40 showed more pronounced changes in expression levels, especially in the left atria, leaning in the direction of overexpression. This tendency is contrary to the ones reported in the referred study, suggesting that the early response of this protein's genetic regulation to atrial pacing can be opposite to the one observed after extended pacing periods (underexpression of Cx40).

The expression regulation of the sodium channel coded by the Scn5a gene is in agreement with similar available studies, like to one by Yue [14] in a dog model of AF. In this study Yue reports significant downregulation of the gene coding for the α subunit of the sodium channel after 7 and 42 days of rapid pacing. The changes reached 42% reduction in mRNA, confirmed by similar, 46.5% reduction in protein concentration after 42 days.
Similar results were reached after much shorter periods of just 4 hours of pacing (see figures 4.3 and 4.4), which confirms the relevance and short term modulation of I_{Na} in atrial ionic remodelling in the rat model. This significant decrease in mRNA if accompanied by similar reduction in the concentration of functional protein, like shown by Yue, can originate low amplitude and low velocity cardiac action potentials.

The genetic expression regulation of Kv4 channel (I_{to}), coded by the Kcnd2 and Kcnd3 genes is investigated in a variety of studies, using several animal models and also humans, and ranging from short to long periods of rapid atrial pacing. Yue in the same study mentioned before [14], reports 71.6% decline in protein concentration of the Kv4.3 specie and 74% in mRNA concentration for the corresponding gene after 42 days of rapid atrial

pacing in dog models of AF.
Bosch et al. [19] show the effects of rapid atrial pacing in the expression of these genes in a rabbit model over periods of 6, 12, 24 and 96 hours. Changes reported by Bosch at 6 and 12 hours are not significant and only a slight reduction was measured for Kv4.3 after 24 hours of pacing.
Yamashita et al. [27] investigated the mRNA and protein concentrations of Kv4.2 and Kv4.3 after periods of pacing raging from 30 minutes to 8 hours in a rat model of AF. Their results show a progressive underespression of the two proteins starting at 1 hour of pacing but only reaching significant values at 2 and 4 hours for the Kv4.2 and Kv4.3 subunits respectively. These results are confirmed by western blot protein quantification analysis. Reduction in Kv4.3 expression was also found in humans with chronic AF [44].

The results found for this genes are shown in figures 4.3 and 4.4 and in general confirm the underexpressin tendency reported in the mentioned studies. The progression is however peculiar and difficult to justify, since the initial underexpression is absent after 2 hours and returns after 4 hours of pacing. Reduction in the expression of these channels and its consequent decrease in I_{to} could in theory prolong the action potential and add to its amplitude, by decreasing the notch repolarization in phase 2 of the cardiac action potential. This is not verified in AF which suggests the influence of other currents in the modulation of action potential duration.

The expression changes of Kv1.5 channel (I_{Kur}) in the context of AF are not consensual over the available literature. Studies in human AF patients [44] show slight underexpression however, the study by Yamashita, referred before, reports significant overexpression right since 30 minutes of pacing, reducing to unchanged expression after 8 hours of pacing, in rats. Other studies [5] report unchanged or underexpression of this channel in models of AF.

In this particular case it cannot be said there is agreement between the measured results and the ones available in the literature since these do not agree between each other. Either way, comparing with the results by Yamashita, in which the experimental conditions are closer related, it can be stated that they disagree almost totally, especially for the right atria.

In the already cited work Bosch el al. studied the expression changes of five subunits of the L-type calcium channel and found most of them to be underexpressed after 6 to 12 hours of atrial pacing. This underexpression was confirmed by matching, although less intense, decreases in protein concentration. Other studies also report pronounced downregulation

of this particular channel over longer periods of time in chronic studies of AF.

The gene coding for this channel was found to be underexpressed at 30 minutes and 4 hours of pacing (figures 4.3 and 4.4), which is in agreement with literature results. However the peculiar progression of the results throughout the three periods of pacing analysed, creates some doubts about this gene's time course of expression regulation. The statistical dispersion of the results also limits the conclusion that can be drawn from these results. Either way the hypothesised reduction in calcium channels would decrease I_{CaL}, which in turn can contribute to a shorter action potential phase 3 plateau and consequent reduced action potential duration and ERP.

The role of the Acetylcholine (Ach) dependent potassium channels in ionic atrial remodelling is still not clear and only a few studies have investigated the expression of these channels in the context of AF. Dobrev et al. [45] have reported downregulation of the Kir3.4 subunit in human patients of chronic AF.
However studies with animal models of AF using rapid atrial pacing show unchanged expression levels of protein subunits of the Ach dependent potassium channels. Although these ion channels expression has found to be unchanged or decreased, the I_{KAch} current was reported augmented. This fact suggests a complex regulation of this kind of current mediated not only by the number of functional proteins.

The results found for the Kcnj3 and Kcnj6 genes coding for Ach dependent potassium channels point in the same underexpression direction as those found in human patients of AF. Although clear underexpression results were found, it is not possible to draw any conclusion about the effect of this reduced expression in the cardiac action potential, since the number of functional channels cannot in this case be connected to the respective current intensities.

It was not possible to find results in the literature concerning the expression of any Cl^- cardiac ion channel, in the context of AF. The calcium currents role in the cardiac action potential is not yet clear, therefore they have not been considered as a contributing factor for atrial remodelling.
These currents are activated mainly by physical stress and exhibit outward rectification, or are predominantly activated at depolarized voltages and, thus, contribute significantly to shortening of the action potential duration. The action potential shortening by Cl^- current activation may not only perpetuate reentry by shortening the refractory period in a reentry pathway, but may also prevent the development of early afterdepolarization and triggered activity caused by the prolongation of action potentials [46].

The initial increase in Cftr expression can be justified by the stress condition of rapid atrial pacing. The pronounced underexpression of this gene after 4 hours of pacing is quite more puzzling, but it can be explained by prolongation of rapid pacing.

The agreement between mRNA and protein concentrations reported in most of the referred studies suggests that, although there are other contributing factors, the reduced transcription is the major mechanism of ion channel downregulation, which characterizes the electrophysiological alterations by which AF leads to its own perpetuation. It also allows the analysis of results based solely on mRNA quantification since an agreement between this parameter and protein concentration can, in most cases, be assumed.

The time periods analysed over this study are insufficient to clarify the phenomena of ionic atrial remodelling, but they add information concerning the early stages of this process. An investigation of the same nature reaching longer periods of rapid atrial pacing would be very useful to clarify the direction of expression regulation. However this kind of long term intervention cannot be accomplished with the same surgical approach, and for that reason an implantable stimulation device is currently being developed by a colleague, that should allow for long term rapid atrial stimulation.

The results presented are quite noisy and statistically disperse, especially the ones concerning the shorter 30 minutes periods, therefore constituting insufficient grounds to draw a clear conclusion from, only an indication of progression can be extracted. The experimental procedures and mRNA quantification analysis were performed in a precise and methodical manner and most probably do not contribute to the dispersion of the results. This problem of statistical dispersion of the two pools analysed can instead be due to inter-individual variability and in that case a possible solution would be to increase the number of subjects. Accounting for this fact an additional set of experiments, comprising one more 5 animal pool, is currently underway, as an attempt to decrease the soaring standard error associated with the quantifications for the first two pools. Another justification for the result dispersion can be the short time scale of the study when compared to the long time scale of the phenomena being analysed. There is no doubt that atrial remodelling is a near immediate phenomena in the sense that changes to the electrophysiological properties of the heart start to happen after only a few minutes of rapid pacing. However, the relevance of the genetic regulation increases in time and the initial changes are most probably not predominantly genetic in nature, but functional.
Several mechanisms interfere in the production and functioning of proteins, and expression regulation is probably not the first one to respond to rapid atrial activation.

Although several studies have demonstrated that mRNA quantification closely correlates with functional protein quantification in the context of long term, chronic rapid pacing experiments, translational and post-translational mechanisms can play an important role in the properties of the final protein, especially in the early stages of exposure to the disturbance, when functional changes can be viewed as the first adaptive response.
In order to account for the translational and post-translational, folding associated mechanisms a proteomics approach would be needed. An immunoblotting study would help to identify the protein subunits that make up the ion channels and probable functional changes that take place in short term adaptation to atrial pacing. In addition, mass spectroscopy methods can be used to quantify the protein species that interfere in the regulation of cardiac ion currents.
The regulatory networks and signaling pathways that control the expression of the ion channels should also be investigated, for in most cases they are the most likely target for pharmacological modulation and are very important for the understanding of the physiological processes of tissue response.

5.2 Signal Measurements

Although the signals measured are not ideal representations of the actual action potential, they present all the properties of a unipolar monophasic action potential, and thus, are approximate illustrations of the action potential, suitable for correlation analysis with any kind of parameter that influences the electrophysiological properties of the tissue.
Recordings from the left atria were attempted, but due to experimental difficulties owing to the inaccessible position of this cavity, these recording had rarely the quality necessary for analysis.
The morphology of this kind of measurement is quite sensitive to variations of the surgical conditions, like position of the heart, position of the electrode in the surface of the heart or conductance variations of the electrode's tip. All these variables are, despite the efforts undertaken, very difficult to control in such minute experimental conditions and are therefore considered as a source of error.
In the clinical environment, this would not be a problem since MAP signals are quite trivial to obtain in a cardiac electrophysiology laboratory. Intracavitary commercially available MAP catheters are introduced in the heart using a peripheral venous access and placed with precision in the desired position to be recorded.

5.3 Signal Analysis

A relatively high number of Gauss function was needed to completely model and fit the morphology of the measured signals. This fact brings problems when it comes to interpret the results due to the high number of produced parameters. Looking solely at the parameters for the Gauss function modelling the main positive deflection of the MAP it is possible to follow the evolution of the signal's shape throughout the different pacing periods.
Unfortunately it is not possible to establish a univocal correspondence between the progression of a given parameter and the expression of a gene. However a possible relation between the overall shape of the action potential, translated by the Gauss function parameters, and the relative expression of the different genes will be explored.
Most of the parameters, excluding DD or width, have an irregular progression from 30 minutes to 4 hours of pacing. This parallels with the time course expression regulation of most of the analysed genes.

The reported results for gene Kcna5 coding for channel Kv1.5 through which flows the ultra rapid outward rectifying I_{Kur} current can be related with the results of some of the Gauss function parameters that model the atrial MAP. This outward current when augmented induces a triangular shaped cardiac action potential, with a less pronounced plateau and decreased duration. Although connection between this particular current and AF remodelling is not clear in the literature, in this case it is possible to correlate the significant underexpression of this gene, after 4 hours of pacing, with the increased kurtosis represented by the parameter CC. Which in turn corresponds to a more square signal, or in the case of the atrial action potential, a more pronounced plateau. The decreased skew represented by the EE parameter at 4 hours can also be correlated with this situation.

Genes Kcnd2 and Kcnd3 which code for Kv4 channel, influence the outward I_{to} current, which in turn has an indirect effect over the cardiac action potential's amplitude. The expected boost in MAP amplitude caused by the decreased expression of I_{to} channels at 30 minutes and 4 hours of pacing, is not corroborated by amplitude changes translated by FF parameter's evolution. These in fact point in the opposite direction.
The amplitude is a parameter greatly influenced by experimental variables, and measures carried out with several hours between them cannot be guaranteed to have happened in the same conditions.

Calcium, specifically the L-type calcium current I_{CaL}, is pointed as the major factor

responsible for the action potential duration, APD, decrease observed in chronic AF remodelling. In this study it was found to be decreased but mainly after 30 minutes of pacing.

In the parametric signal analysis, the DD parameter, which translates de width or duration of the main Gauss function modelling the atrial MAP, is found to be decreased at 30 minutes of pacing, but with a rising tendency, reaching after 4 hours a level superior to control.

Although this tendency is contrary to data presented on chronic studies of AF, it can be related with the expression results for several genes. The Cacna1 gene expression, related with the aforementioned L-type calcium current, is found to be considerably decreased after 30 minutes of pacing returning to near control levels in the other two pacing periods. Also influencing the duration of the cardiac action potential are the Kcnj3 and Kcnj6 genes that code for an acetylcholine dependent inward rectifier potassium channel. These are progressively reduced throughout the three pacing periods. The decreased vagal modulation caused by this fact allows for a raise in APD, counteracting the effect of the calcium and possibly accounting for the observed progressive increase in DD.

The chloride current mediated by the Cftr channel may also play a role in the duration of the cardiac action potential. Amplified I_{Cl} can shorten the action potential and that fact is confirmed in the results for the 30 minutes and 2 hours pacing periods. The role of connexins and I_{Na} is mainly in the action potential's conduction velocity and thus cannot be measured in a single locus action potential recording.

Although the fitting algorithm as shown to be robust and reliable in terms of convergence, the interdependency of the Gauss functions used to model the data greatly complicates the analysis of the results. This problem could be avoided by decreasing the number of interdependable Gauss functions used to model the data. That would imply an increased fitting error if used in signals with complex morphology like to ones recorded in this study, but could be a possible solution in cleaner, more action potential like, MAP signals. In that case only two Gauss functions would be necessary to correctly model and fit the signals.

The relations between genes or groups of genes and a specific Gauss function parameters hypothesized before are deduced by observation of the action potential shape translated by the signal analysis, but cannot be confirmed with the current experimental setup.

In order to isolate the influence of each type of ion current in the morphology of the measured signal, a selective pharmacological blockage of the corresponding ion channels could be used. This way the model parameters associated with the expression changes of each ion channel could be identified.

The investigation of atrial remodelling should take into account the multi-scale dimension of the phenomena, trying to clarify and correlate all the steps, from its genetic or molecular origin to their cellular, tissue or organ manifestations. A complete approach would include the study of signal pathways, genetic regulatory networks and their effects on control of ion channels gene expression, translational and post-translational mechanisms of protein functional modulation, single channel pharmacological blockage to quantify parametrically the influence of each current in the MAP and an experimental pacing setup ranging from short to long periods of atrial stimulation.
A complete study of this kind would require massive resources and expertise in a large number of areas, in a scientific scale quite superior to a master project.

Nowadays treatment strategies for AF include anti-arrhythmic drug therapy, electric cardioversion and surgical ablation, but all three have limitations, for they are aimed at the symptoms of the disease, not at its underlying causes and mechanisms. Anti-arrhythmic drugs are only able to keep patients in sinus rhythm at early stages of AF, once the disease progresses these can lose their effectiveness. Electric cardioversion can stop an AF episode but cannot prevent its recurrence. Finally surgical ablation is a complex procedure effective only in ectopic triggered AF and with variable results in terms of preventing recurrence of AF.
Ideally AF recurrence should be prevented at the early stages of the disease, before it becomes permanent, using therapeutic strategies aimed at the factors and mechanisms that create the atrial conditions for fibrillatory conduction.

Bibliography

[1] WrongDiagnosis.com ^{TM}: http://www.wrongdiagnosis.com/

[2] Paul Khairy and Stanley Nattel: *New insights into the mechanisms and management of atrial fibrillation*, JAMC 29 OCT. 2002; 167(9).

[3] Jeanne M. Nerbonne And Robert S. Kass: *Molecular Physiology of Cardiac Repolarization*, Physiol Rev 85: 1205 – 1253, 2005.

[4] Ralpf F. Bosch, Xiaorong Zeng, Joachim B. Grammer, Katarina Popovic, Christinan Mewis and Volker Kühlkamp: *Ionic mechanisms of electrical remodeling in human atrial fibrillation*, Cardiovascular Research 44 (1999) 121-131

[5] Maurits A. Allessie, Penelope A. Beyden, John Camm, André G. Kléber, Max J. Lab, Marianne J. Legato, Michael R. Rosen, Peter J. Schwartz, Peter M. Spooner, David R. Van Wogoner and Albert L. Waldo: *Pathophysiology and Prevention of Atrial Fibrillation*, Circulation 2001;103;769-777.

[6] Jay Chen, Stephen L. Wasmund and Mohamed H. Hamdan: *Back to the Future: The Role of the Autonomic Nervous System in Atrial Fibrillation*, PACE 2006; 29:413-421.

[7] Kiochiro Kumagai: *Patterns of activation in human atrial fibrillation*, Heart Rhythm, Vol 4, No 3, March 2007.

[8] Andrew L. Wit, Penelope A. Boyden: *Triggered activity and atrial fibrillation*, Heart Rhythm, Vol 4, No 3, March 2007.

[9] Stanley Nattel, Brett Burstein and Dobromir Dobrev: *Atrial Remodeling and Atrial Fibrillation: Mechanisms and Implications*, Circ Arrhythmia Electrophysiol 2008;1;62-73.

[10] Federico Lombardi, Diego Tarricone, Fabrizio Tundo, Federico Colombo, Sebastiano Belletti, Cesare Fiorentini: *Autonomic nervous system and paroxysmal atrial fibrillation: a study based on the analysis of RR interval changes before, during and after paroxysmal atrial fibrillation*, European Heart Journal (2004) 25, 1242-1248.

[11] Kneller J, Zou R, Vigmond EJ, Wang Z, Leon LJ and Nattel S.: *Cholinergic atrial fibrillation in a computer model of a two-dimensional sheet of canine atrial cells with realistic ionic properties*, Circ Res. 2002;90: E73-E87.

[12] Wijffels MC, Kirchhof CJ, Dorland R and Allessie MA.: *Atrial fibrillation begets atrial fibrillation: a study in awake chronically instrumented goats*, Circulation, 1995;92:1954-1968.

[13] Yue L, Feng J, Gaspo R, Li G-R, Wang Z and Nattel S.: *Ionic remodeling underlying action potential changes in a canine model of atrial fibrillation*, Circ Res, 1997;81:512-525.

[14] Yue L, Melnyk P, Gaspo R, Wang Z and Nattel S.: *Molecular mechanisms underlying ionic remodeling in a dog model of atrial fibrillation*, Circ Res, 1999;84:776-784.

[15] Stanley Nattel: *Atrial electrophysiological remodeling caused by rapid atrial activation: underlying mechanisms and clinical relevance to atrial fibrillation*, Cardiovascular Research, 42 (1999) 298-308.

[16] Mohamed Boutjdir, Jean Yves le Heuzey, Thomas Lavergne, Sylvain Chauvaud, Louis Guize and Alain Carpentier: *Inhomogeneity of Cellular refractoriness in Human Atrium: Factor of Arrhythmia?*, Pace, vol 9, December 1986.

[17] S. Nattel, D. Li and L. Yue: *Basic Mechanisms of Atrial Fibrillation-Very New Iinsights Into Very Old Ideas*, Annu. Rev. Physiol. 2000. 62:51-77.

[18] Goette A, Honeycutt C and Langberg JL.: *Electrical remodeling in atrial fibrillation: time course and mechanisms* Circulation 94:2968-74, 1996

[19] Ralph F. Bosch, Constanze R. Scherer, Norman Rüb, Stefan Wöhrl, Klaus Steinmeyer, Hannelore Haase, Andreas E. Busch, Ludger Seipel, Volker Kühlkamp: *Molecular Mechanisms of Early Electrical Remodeling: Transcriptional Downregulation of Ion Channel Subunits Reduces $I_{Ca,L}$ and I_{to} in Rapid Atrial Pacing in Rabbits*, Journal of the American College of Cardiology Vol. 41, No. 5, 2003

[20] Stanley Nattel, Ange Maguy, Sabrina Le Bouter and Yung-Hsin Yeh: *Arrhythmogenic Ion-Channels Remodeling in the Heart: Heart Failure, Myocardial Infarction, and Atrial Fibrillation*, Physiol Rev 87:425 – 456, 2007.

[21] Huub M.W. van der Velden, Jannie Ausma, Martin B. Rook, Anita J.C.G.M. Hellemons, Toon A.A.B. van Veen, Maurits A. Alessie and Habo J. Jongsma: *Gap junctional remodeling in relation to stabilization of atrial fibrillation on the goat*, CArdiovascular Research 46 (2000) 476-486.

[22] Marc Courtemanchea, Rafael J. Ramireza and Stanley Nattel: *Ionic targets for drug therapy and atrial fibrillation-induced electrical remodeling: insights from a mathematical model*, Cardiovascular Research 42 (1999) 477-489.

[23] Vincint Jacquemet, Nathalie Virag and Lukas Kappenberger: *Wavelength and vulnerability to atrial fibrillation: Insights from a computer model of human atria*, Europace, 2005, 7, S83-S92.

[24] L. Wieser, G. Fischer, C.N. Nowak and B. Tilg: *Fibrillatory conduction in branching atrial tissue-Insight from volumetric and monolayer computer models*, Computer Methods and Programs in Biomedicine, 86 (2007) 103-111.

[25] Sandeep V. Pandit, Omer Berenfeld, Justus M.B. Anumonwo, Roman M. Zaritski, James Kneller, Stanley Nattel and José Jalife: *Ionic Determinants of Functional Reentry in a 2-D Model of Human*

Atrial Cells During Simulated Chronic Atrial Fibrillation, Biophysical Journal, Vol 88, june 2005 3806-3821.

[26] Andreas Goette, Uwe Lendeckel and Helmut U. Klein: *Signal transducing systems and atrial fibrillation*, Cardiovascular Research 54 (2002) 247-258.

[27] Takeshi Yamashita, Yuji Murakawa, Noriyuki Hayami, Ei-ichi Fukui, Yuji Kasaoka, Masashi Inoue and Masao Omata: *Short-term effects of rapid atrial pacing on mRNA level of voltage-dependent K^+ channels in rat atrium: electrical remodeling in paroxysmal atrial tachycardia*, Circulation 2000;101:2007-14.

[28] Adolfo A. Leirner, Idágene A. Cestari: *Monophasic Action Potential. New Uses for an Old Technique*, Arq. Bras. Cardiol., volume 72, (n^o 2), 1999.

[29] Jochim K, Katz L.N, Mayne W.: *The monophasic electrogram obtained from the mammalian heart*, American Journal of Physiology (1935) 111:177-186.

[30] JH Levine, EN Moore, AH Kadish, T Guarnieri and JF Spear: *The monophasic action potential upstroke: a means of characterizing local conduction*, Circulation 1986;74;1147-1155.

[31] S. Bertil Olsson: *Atrial repolarization in man. Effect of beta-receptor blockade*, British Heart Journal, I974, 36, 806-810.

[32] MR Franz, K Bargheer, W Rafflenbeul, A Haverich and PR Lichtlen: *Monophasic action potential mapping in human subjects with normal electrocardiograms: direct evidence for the genesis of the T wave*, Circulation 1987;75;379-386.

[33] Alan Kadish: *What is a monophasic action potential?*, Cardiovascular Research 63 (2004) 580-581.

[34] Edward J. Vigmond: *The electrophysiological basis of MAP recordings*, Cardiovascular Research 68 (2005) 502-503.

[35] Franz M.R.: *Method and theory of monophasic action potential recording*, Progress in Cardiovascular Diseases (1991) 33:347-368.

[36] Schütz E.: *Elektrophysiologie des Herzens bei einphasischer Ableitung*, Ergebn Physiol Exper Pharmakol 1936;38:493-620.

[37] Michael R. Franz: *What is a monophasic action potential recorded by the Franz contact electrode?*, Cardiovascular Research 65 (2005) 940-941.

[38] Joseph V. Tranquillo, Michael R. Franz, Björn C. Knollmann, Alexandra P. Henriquez, Doris A. Taylor and Craig S. Henriquez: *Genesis of the monophasic action potential: role of interstitial resistance and boundary gradients*, American Journal of Physiology, Heart and Circulatory Physiology 286:1370-1381, 2004. First published Dec 4, 2003

[39] Masahiko Kondo, Vladislav Nesterenko, Charles Antzelevitch: *Cellular basis for the monophasic action potential. Which electrode is the recording electrode?* Cardiovascular Research 63 (2004) 635-644.

[40] Vladislav V. Nesterenko, Masahiko Kondo, and Charles Antzelevitch: *Biophysical basis for monophasic action potential*, Cardiovascular Research 2005 March 12; 65(4): 942-944.

[41] Michael R. Franz: *Current status of monophasic action potential recording: theories, measurements and interpretations*, Cardiovascular Research 41 (1999) 25-40.

[42] Michiel J. Janse, Tobias Opthof and André G. Kléber: *Animal models of cardiac arrhythmias*, Cardiovascular Research 39 (1998) 165-177

[43] Luís Pina Soares , Raul Carneiro Martins: *Reduced parameter space for reliable clinical identification of the ECG using neural networks and a skewed Gaussian template*, MeMeA 2006, 1-4244-0253-2006 IEEE.

[44] Joachim B. Grammer, Ralph F. Bosch, Volker Kühlkamp and Ludger Seipel: *Molecular Remodeling of Kv4.3 Potassium Channels in Human Atrial Fibrillation*, Journal of Cardiovascular Electrophysiology Vol 11, N0 6, June 2000.

[45] D. Dobrev, E. Graf, E. Wettwer, H. M. Himmel, O. Hála, C. Doerfel, T. Christ, S. Schüler and U. Ravens: *Molecular Basis od Downregulation of G-Portein-Coupled Inward Rectiying K^+ Current (I_K,A_{Ch}) in Chronic Human Atrial Fibrillation: Decrease in GIRK4 mRNA Correlates With Reduced I_K,A_{Ch} and Muscarinic Receptor-Mediated Shortening of Action Potentials*, Circulation 2001; 104;2551-2557.

[46] M Hiraoka, S Kawano, Y Hirano, T Furukawa: *Role of cardiac chloride currents in changes in action potential characteristics and arrhythmias*, Cardiovasc Res (1998) 40: 23-33.

[47] Robert M. Berne, Matthew N. Levy, Bruce M. Koeppen and Bruce A. Stanton: *Physiology, Fifth Edition*,2004, Elsevier Mosby.

[48] biologyclass.neurobio.arizona.edu

[49] http://kvhs.nbed.nb.ca/gallant/biology/action_potential_generation.html

[50] Encyclopædia Britannica, www.britannica.com

[51] Chess GF, Tam RMK, Calaresu FR: *Influence of cardiac neural inputs on rhythmic variations of heart period in the cat.*, Am J Physiol 1975;228:775-780.

[52] Hyndman BW, Kitney RI, Sayers BMcA: *Spontaneous rhythms in physiological control systems.* Nature 1971; 233:339-341.

[53] Pagani M, Lombardi F, Guzzetti S, Rimoldi 0, Furlan R, Pizzinelli P, Sandrone G, Malfatto G, Dell'Orto S, Piccaluga E, Turiel M, Baselli G, Cerutti S, Malliani A: *Power spectral analysis of heart rate and arterial pressure variabilities as a marker of sympathovagal interaction in man and conscious dog.*, Circ Res 1986;59:178-193.

[54] A Malliani, M Pagani, F Lombardi and S Cerutti: *Cardiovascular neural regulation explored in the frequency domain*, Circulation 1991;84;482-492.

[55] Sergio Cerutti, Ary L. Goldberger and Yoshiharu Yamamoto: *Recent Advances in Heart Rate Variability Signal Processing and Interpre-*

tation IEEE TRANSACTIONS ON BIOMEDICAL ENGINEERING, VOL. 53, NO. 1, JANUARY 2006

[56] Task Force of the European Society of Cardiology the North American Society of Pacing Electrophysiology: *Heart Rate Variability, Standards of Measurement, Physiological Interpretation, and Clinical Use*, Circulation. 1996;93:1043-1065.

[57] Raúl Carneiro Martins: *Electrical Signals, Time and Frequency Analysis*, Instrumentation and signal acquisition, Lecture Notes 2005.

[58] Hsiao-Lung Chan, Shih-Chin Fang, Yu-Lin Ko, Ming-An Lin, Hui-Hsun Huang, and Chun-Hsien Lin: *Heart Rate Variability Characterization in Daily Physical Activities Using Wavelet Analysis and Multilayer Fuzzy Activity Clustering*, IEEE TRANSACTIONS ON BIOMEDICAL ENGINEERING, VOL. 53, NO. 1, JANUARY 2006.

[59] J. L. Ducla-Soares, M. Santos-Bento, S. Laranjo, A. Andrade, E. Ducla-Soares, J. P. Boto, L. Silva-Carvalho and I. Rocha: *Wavelet analysis of autonomic outflow of normal subjects on head-up tilt, cold pressor test, Valsalva manoeuvre and deep breathing*,Exp Physiol 92.4 pp 677-686.

Appendix A

Bioelectricity

A.1 Cellular Electrophysiology

In this section a brief overview of the bioelectricity and overall electrical properties of the cell will be made. The basic cell features that allow the generation and propagation of electrical signals will be clarified, namely the cell membrane structure and electrical properties, the ion channels, the resting membrane potential maintenance and the generation of action potentials [47].

Biological membranes as those limiting every cell act as selective permeability barriers. The majority of the molecules present in living systems are highly soluble in water and poorly soluble in the nonpolar environment that exists within the interior of the lipid bilayer of biological membranes. As a consequence, biological membranes pose a formidable barrier to most water soluble molecules, which allows for the maintenance of large concentration differences between the cytoplasm in the interior of the cell and the extracellular fluid in the exterior.

Electrical signals within biological organisms are generally driven by ions, and ions because of their charge are relatively insoluble in the lipid bilayer, and thus the cell membrane is not permeable to most of them. The diffusion of ions across the membrane occurs mainly through protein-mediated membrane transport, where specialized protein ion channels that span the membrane allow for selective permeability to ions (figure A.1). Ion channels can select ions by size or by charge and their operating status, open, closed or inactive can be controlled by the potential difference across the membrane, by mechanical stimulation, by neurotransmitters or other molecules.

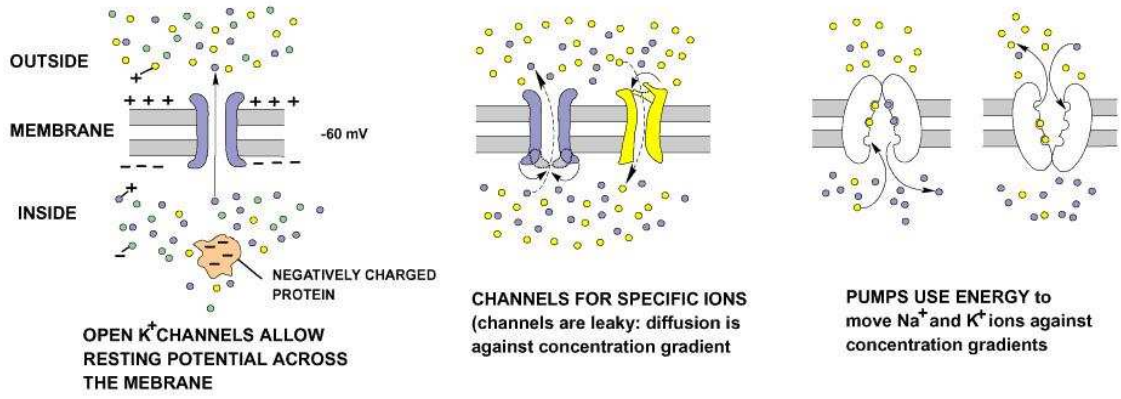

Figure A.1: Ion transporters [48].

The selective affinity of different ion channels for different ions is what gives the membrane its properties of selective permeability, and a specific membrane conductance for each different ion. Some ion channels have the ability to transport substrates against their concentration or electrochemical potential gradients in what is called active transport. This process requires some source of energy, usually from ATP hydrolyzes. These membrane properties are especially important in the case of excitable cells, like neurons and muscle cells.

A.1.1 Ionic Equilibrium and Resting Membrane Potential

Most animal cells maintain an electrical potential difference or voltage across their plasma membranes. Usually this voltage is considered negative regarding the electrically negative cell interior relative to the positive extracellular fluid. The potential difference across the cell membrane in a resting cell is called resting membrane potential and it plays a central role in the excitability of nerve and muscle cells. The resting membrane potential is maintained by an ionic equilibrium between the cell interior and the surrounding fluid.
Two major forces control the equilibria of ions across the cell membrane, the concentration difference and the electrical potential difference. Ions tend to diffuse across permeable membranes according to the gradient of concentration and according to the electrical potential. The quantity that allows us to compare the relative contributions of ionic concentrations and electrical potential to the movement of an ion is called the electrochemical potential (μ) of that ion. The electrochemical potential difference of and ion X^+ across a membrane is defined as:

$$\Delta\mu(X^+) \;=\; \mu_A(X^+) - \mu_B(X^+) \;=\; RTln\frac{[X^+]_A}{[X^+]_B} + zF(E_A - E_B) \qquad \text{(A.1)}$$

Where:

$\Delta\mu$	=	electrochemical potential difference between sides A and B of the membrane
R	=	ideal gas constant
T	=	absolute temperature
$ln\frac{[X^+]_A}{[X^+]_B}$	=	natural logarithm of the concentration ratio of X^+ across the membrane
z	=	charge number of the ion
F	=	Faraday's number
$E_A - E_B$	=	electrical potential difference across the membrane

This equation can be used to calculate the electrical potential differences at equilibrium and to predict the movement of ions in a set of electrochemical conditions.
In most tissues a number of ions are not in equilibrium between the extracellular fluid and the cytoplasm in the interior of the cell. In these conditions each ion will tend to force the transmembrane potential towards its own equilibrium potential, as calculated by the Nernst equitation. The more permeable the membrane is to a specific ion, the greater strength that ion will have in forcing the membrane potential towards its own equilibrium potential.
The interplay of different ion gradients weighted by their specific membrane conductance creates the resting membrane potential and can be illustrated by a very simple mathematical expression. Considering the distribution of three of the most abundant ions in living cells, K^+, Na^+, and Cl^- across the plasma membrane, the transmembrane potential can be predicted by the following equation:

$$E_m \;=\; \frac{g_K}{\sum_g}E_K \;+\; \frac{g_{Na}}{\sum_g}E_{Na} \;+\; \frac{g_{Cl}}{\sum_g}E_{Cl} \qquad \text{(A.2)}$$

Where:

$$\sum_g \;=\; (g_K + g_{Na} + g_{Cl})$$

The expression in Eq.A.2, is called the chord conductance equation, and it states that the transmembrane potential is an average of the electrochemical equilibrium potential of each ion the membrane is permeable to, weighted by the partial membrane conductance for each electrode respectively. This equation clearly shows that the ability of an ion to influence the membrane potential is proportional to the membrane's conductance for that ion. In most resting cells K^+ is the ion with the largest conductance and thus the largest influence in the resting membrane potential.
The charge separation across the membrane maintained by the different ion concentrations, and therefore the resting membrane potential, is disturbed whenever there is a net flux of ions into or out of the cell. A reduction of the charge separation is called depolarization; an increase in charge separation is called hyperpolarization.

A.1.2 Generation and Conduction of Action Potentials

Electrical signals are all caused by transient changes in the current flow into and out of the neuron, which drives the electrical potential across the plasma membrane away of its resting condition. Neurons communicate with one another and with muscle fibers by means of nerve action potentials, but this phenomenon can also take place in other types of conducting tissue like the cardiac muscle.
The previously described resting membrane potential creates the initial cell conditions for the generation and conduction of an action potential. An action potential is a rapid, transient, change in the transmembrane potential difference followed by a return to the resting membrane potential.

Whenever the cell's resting membrane potential is disturbed by a transient depolarizing potential, such as an excitatory synaptic potential, the resultant decrease in the membrane potential activates the voltage-dependent Na+ channels. The activation of the Na^+ channels in turn increases the membrane's Na^+ permeability resulting in a Na^+ influx which accelerates the depolarization process, producing the rising phase of the action potential. This positive feedback cycle, develops exponentially driving the membrane potential toward the positive values. The rise of the membrane potential ultimately triggers the process of Na^+ channel inactivation, which prevents further membrane depolarization.
The following repolarization process results from the delayed opening of voltage gated K^+ channels. As K^+ channels begin to open, K^+ efflux increases. The delayed increase in K^+ efflux combined with a decrease in Na^+ influx to produce a net efflux of positive

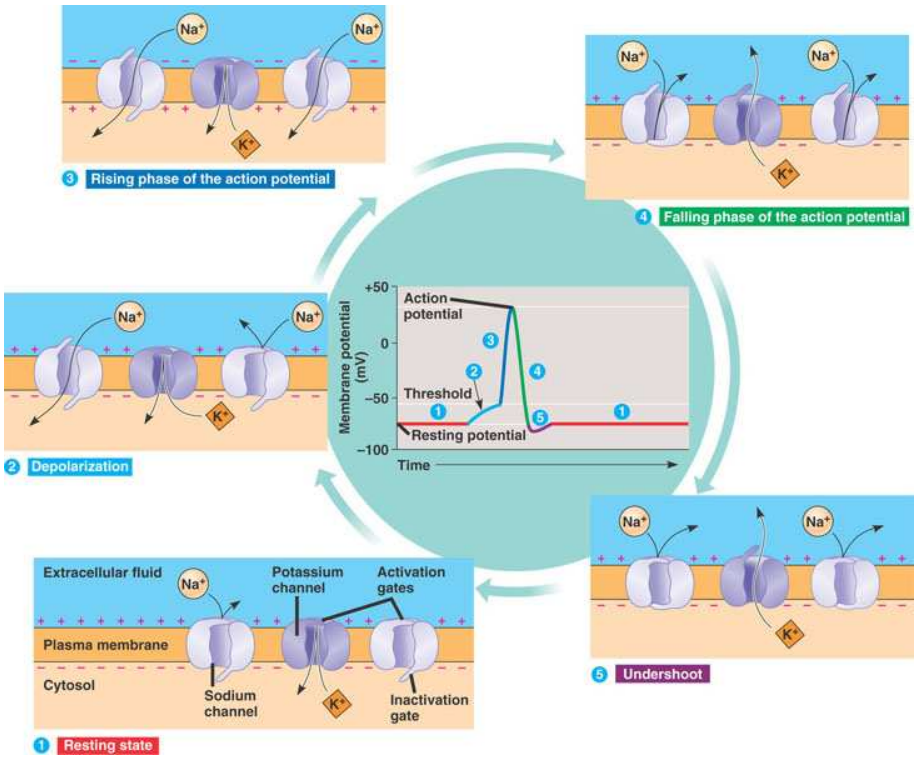

Figure A.2: Action Potential Generation [49].

charge from the cell, which produces the falling phase of the action potential and the afterhyperpolarization, finally returning the cells to its resting potential. This process is illustrated in figure A.2.

This process results in a wave of depolarization/repolarization that can propagate all over the surface of the cell's axon (figure A.3). Once the depolarization/repolarization wave reaches the axon terminal it turns on the mechanisms of synaptic transmission which results in the necessary communication between nerve cells.
Action potentials are all-or-nothing events. All action potentials in a determinate cell are the same size. If the disturbing potential is below a certain threshold level, no action potential occurs. If it is above threshold level, the cell is always depolarized to the same level.

During much of the action potential the membrane is completely refractory to further stimulation. In these conditions it is unable to fire a second action potential no matter how strongly the cell is stimulated. This unresponsive state is called absolute refractory period. The cell is refractory because a large fraction of its Na+ channels is voltage inactivated and cannot be reopened until the membrane is repolarized.

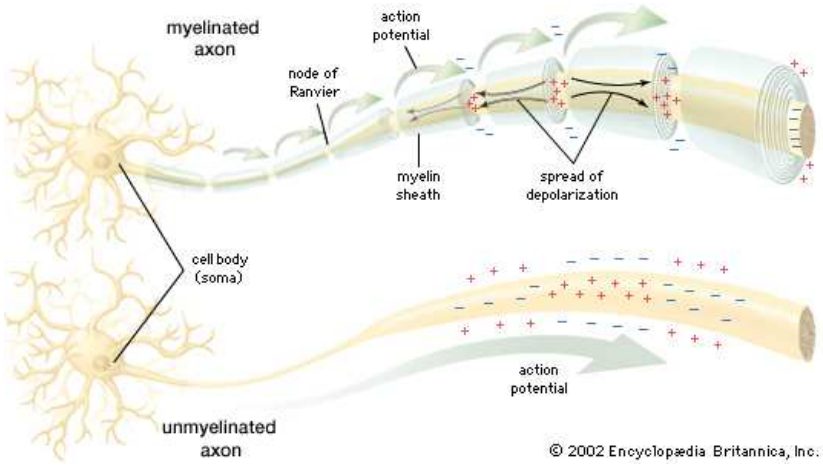

Figure A.3: Action Potential Propagation [50].

During the latter part of the action potential the cell is able to fire a second action potential but a stronger then normal stimulus is required. This period is called relative refractory period. During this period some Na^+ channels are still voltage inactivated, therefore a stronger stimulus is needed to open the critical number of Na+ channels necessary to trigger an action potential. Throughout the relative refractory period the conductance to K^+ is elevated in order to repolarize the membrane, which further opposes a new depolarization of the membrane.

During a complete action potential the plasma membrane of an axon climbs from its resting potential of -70mV to near 40mV and back to -70mV in about 5ms and it can travel along the axon at conduction speeds as fast as 100m/s. Because they are able to transmit information so fast, the flow of action potentials is a very efficient form of data transmission.

Appendix B

Autonomic Nervous System

The nervous system consists of two main structures, the central nervous system, in which are included the brain and the spinal cord and the peripheral nervous system comprised by the sense organs and the nerves linking the sense organs, muscles, and glands to the central nervous system. The structures of the peripheral nervous system are further subdivided into the autonomic nervous system and the somatic nervous system.

The autonomic nervous system (ANS) is a part of the peripheral nervous system that functions to regulate the basic visceral processes needed for the maintenance of normal bodily functions and homeostasis. It has an important function in maintaining the internal environment of the human body in a steady state. This role is vital in returning the body to a homeostatic state after trauma and also to cope with and adapt to everyday changes.

As various changes occur within the environment, both internal and external, the autonomic nervous system reacts by regulating internal variables such as the blood pressure, heart rate, concentration of salts in the blood stream, among others. This process of change in internal parameters to adapt to external variations is called allostasis, and it is an evolution of the concept of homeostasis.

The system operates independently of voluntary control, hence the name which comes from ancient Greek meaning ’self governing’, although certain events, such as emotional stress, fear, sexual excitement, and alterations in the sleep-wakefulness cycle, change the level of autonomic activity.

Once physiologists believed that the system was wholly independent of the central nervous system. However we now realize that this is not quite the picture and that there is some central nervous system components involved. This includes the spinal cord, the brain stem and the hypothalamus. The hypothalamus is probably the most important area of the brain involved with the ANS but other areas such as the medulla oblongata and

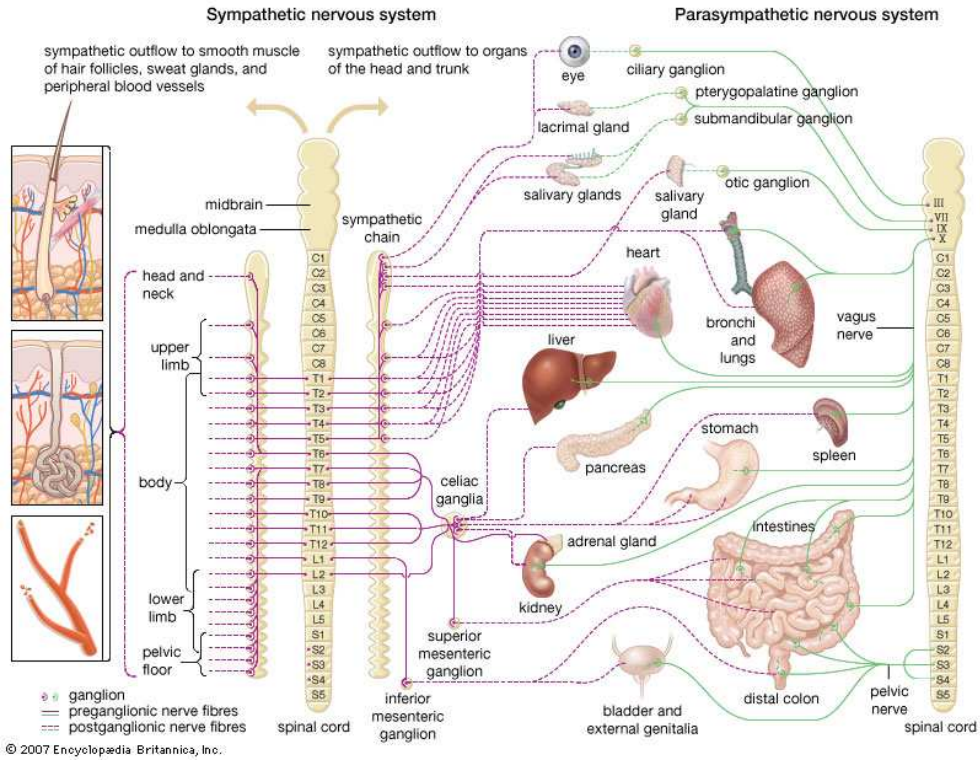

Figure B.1: Autonomic Nervous System [50].

parts of the limbic system of the cerebral cortex have an important part to play.

The ANS consists of a somatic afferent pathway, a central nervous system integrating complex (brain and spinal cord), and two efferent limbs, the sympathetic and the parasympathetic nervous systems. Norepinephrine is the primary chemical neurotransmitter at sympathetic nerve endings, whereas acetylcholine is the primary chemical neurotransmitter at parasympathetic nerve endings. Acetylcholine, catecholamines (dopamine, etc.) and several other peptides further modulate the system centrally in the brainstem and hypothalamus.

The ANS is usually defined as a motor system that innervates three major types of tissue, cardiac muscle, smooth muscle, and glands. However, this definition needs to be expanded to encompass the fact that it also relays visceral sensory information, coming from just about all organs, into the central nervous system and processes it in such a way as to make alterations in the activity of specific autonomic motor outflows, such as those that control the heart, blood vessels, and all visceral organs. It also causes the release of hormones involved in energy metabolism (*e.g.*, insulin, glucagon, epinephrine) or cardiovascular functions (*e.g.*, renin, vasopressin). These integrated responses maintain the normal internal environment of the body in equilibrium and allow it to adapt to external

or internal changes.

The ANS consists of two major divisions, the sympathetic nervous system and the parasympathetic nervous system. These often function in antagonistic ways. However it is important to remember that they all form part of an integrated whole and that both the sympathetic nervous system and the parasympathetic nervous system are operating continuously along with the rest of the nervous system. They are continually responding in varying degrees to information provided by the sensory component of the nervous system. However the sympathetic division dominates during stressful times and the parasympathetic division dominates during times of emotional calm and/or physical rest.

The motor outflow of both systems is formed by two serially connected sets of neurons. The first set, called preganglionic neurons, originates in the brain stem or the spinal cord, and the second set, called ganglion cells or postganglionic neurons, lies outside the central nervous system in collections of nerve cells called autonomic ganglia. Parasympathetic ganglia tend to lie close to or within the organs or tissues that their neurons innervate, whereas sympathetic ganglia lie at a more distant site from their target organs. Both systems have associated sensory fibers that send feedback information into the central nervous system regarding the functional condition of target tissues.

Unlike the somatic nervous system, which always excites muscle tissue, the ANS can either excite or inhibit innervated tissue. Most associated tissues and organs have nerves of both the sympathetic and the parasympathetic nervous systems. The two systems can stimulate the target organs and tissues in opposite ways, such as sympathetic stimulation to increase heart rate and parasympathetic to decrease heart rate, or the sympathetic stimulation resulting in pupil dilation, and the parasympathetic in pupil constriction. Or, they can both stimulate activity in concert, but in different ways, such as both increasing saliva production by salivary glands, but with sympathetic stimulation yielding viscous or thick saliva and parasympathetic yielding watery saliva.

In general, the ANS controls homeostasis, which is the constancy of the content of tissues in gases, ions, and nutrients. It does so mostly by controlling cardiovascular, digestive, and respiratory functions, but also salivation, perspiration, diameter of the pupils, micturition (the discharge of urine), and erection. While many of the activities of the ANS are involuntary, breathing, for example, can be in part consciously controlled. This example, among others, illustrates that the so-called “autonomic nervous system” is not truly autonomous. It is anatomically and functionally linked to the rest of the nervous system and a strict delineation is impossible.

B.1 Sympathetic nervous system

Sympathetic preganglionic neurons originate in the lateral horns of the 12 thoracic and the first 2 or 3 lumbar segments of the spinal cord. For this reason the sympathetic system is sometimes referred to as the thoracolumbar outflow. The axons of these neurons exit the spinal cord in the ventral roots and then synapse on either sympathetic ganglion cells or specialized cells in the adrenal gland.

Sympathetic preganglionic neurons originate in the lateral horns of the 12 thoracic and the first 2 or 3 lumbar segments of the spinal cord. For this reason the sympathetic system is sometimes referred to as the thoracolumbar outflow. The axons of these neurons exit the spinal cord in the ventral roots and then synapse on either sympathetic ganglion cells or specialized cells in the adrenal gland. Sympathetic ganglia can be divided into two major groups, paravertebral and prevertebral (or preaortic), on the basis of their location within the body. Paravertebral ganglia generally lie on each side of the vertebrae and are connected to form the sympathetic chain or trunk. There are usually 21 or 22 pairs of these ganglia: 3 in the cervical region, 10 to 11 in the thoracic region, 4 in the lumbar region, 4 in the sacral region, and a single, unpaired ganglion lying in front of the coccyx called the ganglion impar. The three cervical sympathetic ganglia are the superior cervical ganglion, the middle cervical ganglion, and the cervicothoracic ganglion (also called the stellate ganglion). The superior ganglion innervates viscera of the head; the middle and stellate ganglia innervate viscera of the neck, thorax (i.e., the bronchi and heart), and upper limb. The thoracic sympathetic ganglia innervate the trunk region, and the lumbar and sacral sympathetic ganglia innervate the pelvic floor and lower limb. All the paravertebral ganglia provide sympathetic innervation to blood vessels in muscle and skin, arrector pili muscles attached to hairs, and sweat glands.

The three preaortic ganglia are the celiac, superior mesenteric, and inferior mesenteric. Lying on the anterior surface of the aorta, they provide axons that are distributed with the three major gastrointestinal arteries arising from the aorta. The celiac ganglion innervates the stomach, liver, pancreas, duodenum, and the first part of the small intestine; the superior mesenteric ganglion innervates the small intestine and the inferior mesenteric ganglion innervates the descending colon, sigmoid colon, rectum, urinary bladder, and sexual organs.

B.2 Parasympathetic nervous system

The parasympathetic nervous system is organized in a manner similar to the sympathetic nervous system. Its motor component consists of a two-neuron system. The preganglionic neurons lie in specific cell groups (also called nuclei) in the brain stem or in the lateral horns of the spinal cord at sacral levels (segments S2-S4). Because parasympathetic fibers exit from these two sites, the system is sometimes referred to as the craniosacral outflow. Preganglionic axons emerging from the brain stem project to parasympathetic ganglia that are located in the head (ciliary, pterygopalatine [also called sphenopalatine], and otic ganglia) or near the heart (cardiac ganglia), embedded in the end organ itself (e.g., the trachea, bronchi, and gastrointestinal tract), or situated a short distance from the urinary bladder (pelvic ganglion). Both pre- and postganglionic neurons secrete acetylcholine as a neurotransmitter, but, like sympathetic ganglion cells, they also contain other neuroactive chemical agents that function as cotransmitters.

The parasympathetic nervous system modulates mainly visceral organs such as glands. These are never activated en masse as in the “fight or flight” sympathetic response.

The third cranial nerve (oculomotor nerve) contains parasympathetic nerve fibers that regulate the iris and lens of the eye. From their origin in the Edinger-Westphal nucleus of the midbrain, preganglionic axons travel to the orbit and synapse on the ciliary ganglion. The ciliary ganglion contains two types of postganglionic neurons: one innervates smooth muscle of the iris and is responsible for pupillary constriction, and the other innervates ciliary muscle and controls the curvature of the lens.

Various secretory glands located in the head are under parasympathetic control. These include the lacrimal gland, which supplies tears to the cornea of the eye; salivary glands (sublingual, submandibular, and parotid glands), which produce saliva; and nasal mucous glands, which secrete mucus throughout the nasal air passages. The parasympathetic preganglionic neurons that regulate these originate in the reticular formation of the medulla oblongata. One group belongs to the superior salivatory nucleus and lies in the rostral part of the medullary reticular formation. These neurons send axons out of the medulla in a separate part of the seventh cranial nerve (facial nerve) called the intermediate nerve. Some of the axons innervate the pterygopalatine ganglion, and others project to the submandibular ganglion. Pterygopalatine ganglion cells innervate the vasculature of the brain and eye as well as the lacrimal gland, nasal glands, and palatine glands, while neurons of the submandibular ganglion innervate the submandibular and sublingual salivary glands. A second group of parasympathetic preganglionic neurons

belongs to the inferior salivatory nucleus, a group lying in the caudal part of the medullary reticular formation. Its neurons send axons out of the medulla in the ninth cranial (glossopharyngeal) nerve and to the otic ganglion. From this site, postganglionic fibers travel to and innervate the parotid salivary gland.

Preganglionic parasympathetic fibers of the tenth cranial nerve (vagus) arise from two different sites in the medulla. Neurons that slow heart rate arise from a part of the ventral medulla called the nucleus ambiguus, while those that control the gastrointestinal tract arise from the dorsal vagal nucleus. After exiting the medulla in the vagus nerve and traveling to their respective organs, the fibers synapse on ganglion cells embedded in the organs themselves. The vagus nerve also contains visceral afferent fibers that carry sensory information from organs of the neck (larynx, pharynx, and trachea), chest (heart and lungs), and gastrointestinal tract into a visceral sensory nucleus located in the medulla and called the solitary tract nucleus.

A third division of the autonomic system, termed the enteric nervous system, consists of a collection of neurons embedded within the wall of the entire gastrointestinal tract and its derivatives. This system controls gastrointestinal motility and secretions.

B.3 Autonomic Cardiovascular Control

This section will focus on the autonomic control of cardiovascular parameters, specifically, heart rate and blood pressure and the tools used to assess these control variables.
An individual's heart rate is constantly changing is response to the metabolic requirements of the body or changes in the environment that cause or alleviate stress. Various intrinsic, neural, and hormonal factors act to influence the rhythm control and impulse conduction within the heart. The rhythmic control of the cardiac cycle and its accompanying heartbeat relies on the regulation of impulses generated and conducted within the heart. The sympathetic and parasympathetic divisions of the autonomic system regulate heart rhythm by affecting the same intrinsic impulse conducting mechanisms that lie within the heart in opposing ways.
Extrinsic control of the heart rate and rhythm is achieved via ANS impulses (regulated by the medulla oblongata) and specific hormones that alter the contractile and or conductive properties of heart muscle. In very simple terms, the sympathetic division of the ANS works, via the cervical sympathetic chain ganglia, to increase the heart rhythm and contractibility in situations of stress or increased metabolic demand. In contrast the

parasympathetic division of the ANS works, via the vagal nerve, to decrease heart rhythm and contractibility in situations of decreased metabolic demand. Sympathetic stimulation also increases the conduction velocity of cardiac muscle fibers. Parasympathetic stimulation decreases conduction velocity. The regulation in impulse conduction results from the fact that parasympathetic fibers utilize acetylcholine as a neurotransmitter hormone that alters the transmission of the action potential by altering membrane permeability to specific ions (e.g., potassium ions K^+). In contrast, sympathetic postganglionic neurons secrete the neurotransmitter norepinephrine that alters membrane permeability to sodium (Na^+) and calcium ions (Ca^{2+}).
In this apparently simple detail resides the reason why is the ANS an important factor to have into consideration in this study. Its role in atrial fibrillation as, for a long time, been a matter of discussion and although there is not an agreement on the mechanisms by which the ANS interferes in AF, the simple fact that it influences the cardiac ionic currents, justifies the investigation of the autonomic cardiovascular parameters.

Vasomotion, and consequently, blood pressure is controlled in a similar way by the ANS, predominantly by the sympathetic division.
The constant changes in heart rate and blood pressure observed in normal ECG and blood pressure continuous recordings are thought to be an effect of constant autonomic cardiovascular regulation, trough the balance of sympathetic and vagal outflows.

It was found that these modulating influences have specific rhythms [51, 52], characterized by a low frequency (LF) component mainly determined by the sympathetic nervous system, and a high frequency (HF) component mainly determined by the parasympathetic nervous system, or vagal outflow in the particular case of heart rate [53]. Other rhythms like respiration fall into the same range of frequencies, often influencing the quantification of sympathovagal balance.
The LF and HF peaks differ among species, each having two frequency bands where the peaks are more probable to fall into, among individuals and even for the same person in different occasions.

The assumption that it is possible to measure autonomic modulation from non-invasive recordings motivated the development of several methods to evaluate and even quantify the relative influence of the sympathetic and parasympathetic divisions of the ANS, in cardiovascular function in what is called heart rate variability analysis [54, 55, 56]. The range of this matter is such that over the past 30 years, heart rate variability (HRV) has become a central topic in physiological signal analysis, serving as a vital noninvasive indicator of cardiovascular and autonomic system function, with direct connections to

respiratory, central nervous and metabolic dynamics and huge clinical repercussions over a variety of specialties.

Several methods have been proposed to analyse HRV in the time and frequency domains. The most popular and widely spread method throughout the clinical and research environments is the Fourier analysis. However recently other frequency analysis tools have came about with promising new features that can overcome some of the limitations of the good old Fourier transform.

All frequency based methods of analyzing the HRV are applied to the tachogram, which is a time series of successive R-R wave distance, thus representing for each heart beat the heart period.

The Fourier transform evaluates the frequency content of a signal at all time instances, disregarding any variations of frequency content. This fact constitutes one of the major limitations of Fourier analysis; it is suitable for stationary signals [1] only. The frequency spectrum provided by the Fourier transform contains information about all the frequencies that occur in the signal, but no indication on the moment they occur.
The stationarity requisite can be somewhat bended. Stationarity can be assumed for small segments of the non-stationary signal at hand. This leap to stationarity also overcomes the time resolution constraint the Fourier transform, which by being applied to segments instead of the entire signal, generates a artificial time resolution of the frequency spectrum. This method is called the Short Time Fourier Transform.
Using this method entails a compromise, for the time resolution earned by decreasing the duration of the analysed segments, and with it the number of samples used, is paid in the form of a decrease in frequency resolution of the spectrum [57]. This inverse dependence between number of samples and frequency resolution constitutes one of the major limitations of the Fourier transform.

One of the methods that overcome some of the limitations of the Fourier transform is the Wavelets transform [58].
The wavelet transform is a frequency analysis method developed as an alternative to Fourier analysis, specifically to the Short Time Fourier Transform and its resolution related problems. The most interesting feature of the Wavelet transform is its time and frequency resolution properties. In the wavelet transform time and frequency resolution are variable and adaptable, there is high time resolution and low frequency resolution for high frequencies, and low time resolution and high frequency resolution for low

[1] Stationary signal: signal with constant frequency content.

frequencies. This means higher frequencies are better resolved in time, and lower frequencies are better resolved in frequency. Like the Fourier transform also the wavelets transform can be reversed in order to synthesize the original signal from its coefficients. The more normally used version of Wavelet analysis is the discrete version of the wavelets transform. The discrete wavelets transform works by consecutive filtration of the signal, and consequent division into components of different frequencies or scales. These components are then grouped in order to define the interest, LF and HF, frequency bands and finally the transform is reversed in order to synthesize the original signal components that fall into the LF and HF frequency bands [59].